

Review

A Review of Cobalt-Containing Nanomaterials, Carbon Nanomaterials and Their Composites in Preparation Methods and Application

Hongfeng Chen, Wei Wang, Lin Yang, Liang Dong, Dechen Wang, Xinkai Xu , Dijia Wang, Jingchun Huang, Mengge Lv and Haiwang Wang *

A Key Laboratory of Dielectric and Electrolyte Functional Material Hebei Province, Northeastern University at Qinhuangdao, Qinhuangdao 066004, China; chf1405104586@126.com (H.C.); wang15991035831@163.com (W.W.); yl20010508@yeah.net (L.Y.); dongliang@neuq.edu.cn (L.D.); aaa1291233239@163.com (D.W.); autxxk@163.com (X.X.); dijia8121@foxmail.com (D.W.); hjc13799078806@163.com (J.H.); doublelmg@outlook.com (M.L.)

* Correspondence: whwdbdx@126.com

Abstract: With the increasing demand for sustainable and green energy, electric energy storage technologies have received enough attention and extensive research. Among them, Li-ion batteries (LIBs) are widely used because of their excellent performance, but in practical applications, the electrochemical performance of electrode materials is not satisfactory. Carbon-based materials with high chemical stability, strong conductivity, high specific surface area, and good capacity retention are traditional anode materials in electrochemical energy storage devices, while cobalt-based nanomaterials have been widely used in LIBs anodes because of their high theoretical specific capacity. This paper gives a systematic summary of the state of research of cobalt-containing nanomaterials, carbon nanomaterials, and their composites in LIBs anodes. Moreover, the preparation methods of electrode materials and measures to improve electrochemical performance are also summarized. The electrochemical performance of anode materials can be significantly improved by compounding carbon nanomaterials with cobalt nanomaterials. Composite materials have better electrical conductivity, as well as higher cycle ability and reversibility than single materials, and the synergistic effect between them can explain this phenomenon. In addition, the electrochemical performance of materials can be significantly improved by adjusting the microstructure of materials (especially preparing them into porous structures). Among the different microscopic morphologies of materials, porous structure can provide more positions for chimerism of lithium ions, shorten the diffusion distance between electrons and ions, and thus promote the transfer of lithium ions and the diffusion of electrolytes.

Keywords: cobalt-containing nanomaterials; carbon nanomaterials; composite materials; anode of lithium-ion batteries



Citation: Chen, H.; Wang, W.; Yang, L.; Dong, L.; Wang, D.; Xu, X.; Wang, D.; Huang, J.; Lv, M.; Wang, H. A Review of Cobalt-Containing Nanomaterials, Carbon Nanomaterials and Their Composites in Preparation Methods and Application. *Nanomaterials* **2022**, *12*, 2042. <https://doi.org/10.3390/nano12122042>

Academic Editor: Nikos Tagmatarchis

Received: 7 May 2022

Accepted: 7 June 2022

Published: 14 June 2022

Publisher's Note: MDPI stays neutral with regard to jurisdictional claims in published maps and institutional affiliations.



Copyright: © 2022 by the authors. Licensee MDPI, Basel, Switzerland. This article is an open access article distributed under the terms and conditions of the Creative Commons Attribution (CC BY) license (<https://creativecommons.org/licenses/by/4.0/>).

1. Introduction

With the continuous development of the times, fossil fuels, which are non-renewable resources, are decreasing day by day, and the environmental pollution problem is becoming more and more serious. It is extremely urgent to develop green renewable energy, such as wind energy and solar energy [1]. Because these energy sources are highly dependent on the natural environment, their transfer and storage become particularly important. Therefore, researchers and the energy community are very interested in the research of more efficient energy storage devices and technologies. At present, rechargeable batteries and supercapacitors are the main chemical energy storage devices. Among them, rechargeable lithium-ion batteries with fast charging and discharging speed, high energy density, high voltage, and good safety performance have been widely used in digital products, such as mobile phones and notebook computers.

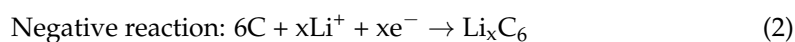
Compared with traditional materials, nanostructured electrodes have the advantages of improving highly reversible lithium insertion ability, reducing diffusion length, increasing lithiation/delithiation rates, and enhancing electrical conductivity. Carbon nanomaterials represent one of the most widely studied nanomaterials at present. Because of their novel structures, mechanical properties, and electronic double layer capacitor (EDLC) behavior, most nano-carbon-based anode materials that have been developed have remarkable lithium storage and recycling properties compared with commercial graphite. The theoretical capacity of commercial graphite is 372 mA h g^{-1} , and the rate performance is very limited. In addition, carbon nanomaterials also have excellent electrical and mechanical properties, so they show great application potential in LIBs, and are considered as the most commercial anode materials in lithium-ion batteries [1,2]. With the continuous exploration of researchers, it has been found that transition metal compounds with the Faraday charge transfer process can store more energy than carbon-based materials, and the reversible capacity of transition metal oxides (MO, where M = Fe, Co, Ni or Cu) is almost three times that of graphite, forcing their consideration as a promising electrode material [3,4]. Among these transition metal compounds, cobalt nano compounds, including cobalt oxides, hydroxides, sulfides, phosphates, selenides, and other derivatives, are widely used in lithium-ion batteries because of their high theoretical specific capacitance. However, most cobalt-based electrode materials are prone to large volume fluctuation during use. Due to the absorption and release of Li^+ , the electrode materials are finally crushed and separated from the current collector, which can greatly attenuate their capacity and deteriorate their recyclability. One of the ways to solve this problem is to combine carbon nanomaterials to prepare composite materials with special structure.

Up to now, there have been many reports about cobalt-based electrode materials and carbon nanomaterials in lithium-ion battery anodes. However, most of these reports introduce them separately, and there is no overview of these two materials and their composites in lithium-ion battery anodes at present. Therefore, the recent research progress of cobalt nanomaterials, carbon nanomaterials, and their composites in lithium-ion batteries is reviewed in this paper. The working mechanism of the lithium-ion battery and the application of cobalt nano-materials, carbon nano-materials, and their composite materials in lithium-ion battery anode is discussed respectively. Finally, the challenges of electrode materials at present are discussed.

2. Application of Cobalt-Based Nanomaterials

With the development of economy and society, people's demand for sustainable and renewable energy is increasing day by day. In this context, power storage technology develops rapidly [5]. LIBs are widely used in green vehicles and portable electronic devices due to their high energy density, environmental friendliness, long cycle life, and almost no memory effect. Currently, lithium-ion batteries are at the forefront of current energy storage material research.

The LIBs are mainly composed of a positive electrode, negative electrode, electrolyte, and separator. The working mechanism of LIBs is the reversible intercalation and delamination of lithium ions between the positive and negative electrodes [6], thereby forming a lithium ion concentration difference between the positive and negative electrodes, and then charging and discharging through the gain and loss of electrons. As shown in Figure 1, in LiCoO_2 -graphite Li-ion batteries, lithium ions are deintercalated from the LiCoO_2 electrode and inserted into the negative electrode (graphite) through the electrolyte and separator, which is the charging process. At this time, Co^{3+} undergoes an oxidation reaction and becomes Co^{4+} , and the lost electrons are transferred to the negative electrode by means of an external circuit. The discharge reaction and the charge reaction are reciprocal. The electrode reaction formulas of the lithium-ion battery during the charging process are as follows [7]:



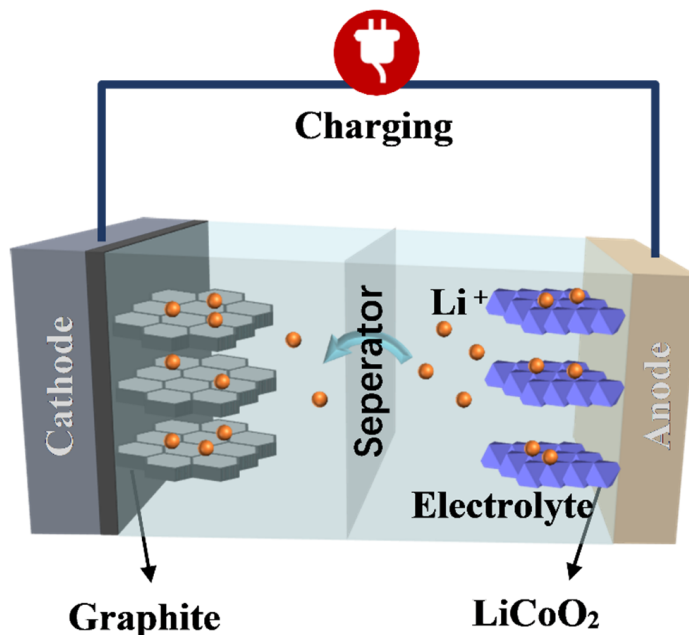
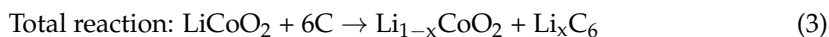


Figure 1. Schematic diagram of lithium-ion battery charging process.

At present, commercial lithium-ion batteries usually use 4 V cathode materials, such as spinel LiMn_2O_4 , olivine LiFePO_4 , and layered $\text{LiNi}_{1/3}\text{Mn}_{1/3}\text{Co}_{1/3}\text{O}_2$ or LiCoO_2 . However, their energy density is limited, and the energy density of olivine LiFePO_4 is only 120 W h kg^{-1} [8]. In recent decades, LCO (LiCoO_2) invented by Sony has been widely used in the battery field. However, LCO is unstable in a wide range of de-lithiated state. Overcharge reaction of lithium-ion battery will change the positive electrode structure, make the material have strong oxidizability, and easily make the solvent in electrolyte oxidize strongly. Moreover, this effect is irreversible, and the large accumulation of heat released by the reaction will cause the risk of thermal runaway. Therefore, the LCO battery is not the first choice for automobiles [9]. When the charging voltage of the LCO-based battery is higher than 4.35 V, the reaction between the electrolyte solvent and the highly oxidized LCO cathode surface will occur, resulting in the instability of the electrode structure and capacity attenuation and increasing the interface impedance. To address this problem, Liu et al. developed a doping technique to solve its long-term instability, explored the co-doping of LCO with lanthanum and aluminum, and proved that doping La and Al on cobalt-containing precursors can improve the structural stability and Li^+ diffusion rate of LiCoO_2 . This doped LiCoO_2 shows an extremely high capacity of 190 mA h g^{-1} , achieving a capacity retention rate of 96% and significantly improving its structural stability during 50 cycles of 4.5 V cutoff voltage [10].

The commonly used electrode material on the anode side is graphite, which has a relatively low theoretical capacity (372 mA h g^{-1}) for commercial LIBs [11], and also suffers from the disadvantage of flammability [12].

Due to the practical demands in life, high energy density and power density are required to perform well in energy storage devices [12]. Although LIBs have a high energy density to a certain extent, there are still some problems, such as low power density, safety problems, and material aging, etc., which will limit their practical application [13]. Therefore, scholars have extensively explored the development of new electrode materials to improve the energy density and power density of lithium-ion batteries and to improve their comprehensive electrochemical performance.

In addition, a large number of experimental studies have proved that compounding cobalt nano-compounds with other materials to construct different structures plays an im-

portant role in improving the electrochemical performance of single cobalt nano-materials and has significant advantages in electrochemical energy storage devices. For example, Aboelazm et al. prepared Co_3O_4 with excellent performance by electrodeposition using magnetic field effects [14]. The specific capacitance of the Co_3O_4 nanostructure is very high (1273 F g^{-1}), which is four times that of the Co_3O_4 nanomaterial prepared without magnetic field effect (315 F g^{-1}). Such a high charge storage is due to the higher electroactive surface area contributing to faster ion diffusion and redox reactions, thus improving the pseudo capacitance in the Co_3O_4 nanostructure. The stability of the Co_3O_4 nanostructure reaches 96% after 5000 cycles, which is due to the presence of easily diffusible ions in the layered nanostructure. Ali et al. prepared $\text{Co}_3\text{O}_4/\text{SiO}_2$ nanocomposites following the citric acid-gel method [15]. Microscopically, Co_3O_4 nanoparticles were uniformly embedded in SiO_2 matrix. The electrochemical analysis results show that the prepared $\text{Co}_3\text{O}_4/\text{SiO}_2$ nanocomposites have good charge storage properties (1143 F g^{-1} at 2.5 mV s^{-1} ; 679 F g^{-1} at 1 A g^{-1}), which is due to the easy infiltration of electrolyte in SiO_2 matrix and redox reaction with Co_3O_4 electroactive surface. After 900 times of continuous charge and discharge, the capacitance retention rate is higher than 92%, indicating that the composite has good stability. Furthermore, Ali et al. prepared activated carbon by using the CaO impregnation method with palm kernel shell (ACPKS) as raw material, and then prepared CaO/ACPKS with highly porous honeycomb structure with egg shell waste as raw material [16]. The specific capacitance of CaO/ACPKS at 0.025 A g^{-1} is up to 222 F g^{-1} , which is about three times that of ACPKS. This is because the CaO/ACPKS structure stores more charge through ion intercalation/deintercalation, and the nano aperture is beneficial to the adsorption of ions on the supercapacitor.

A large number of studies have shown that the composite of cobalt compounds and carbon nanomaterials can significantly improve the electrochemical performance of lithium-ion batteries [17–20]. For example, in the research of Minakshi et al., LiCoPO_4/C nanocomposites were prepared by solid-state fusion [21]. The introduction of amorphous carbon coating can improve the electrical conductivity and electrochemical performance. The tests show that the initial discharge capacity of the synthesized LiCoPO_4/C nanocomposites reaches 123 mA h g^{-1} , and the capacity retention is 89% after 30 cycles. Kang et al. prepared a $\text{CoOHCl}@\text{C}$ composite with egg-like structure, in which cobalt hydroxychloride is used as egg yolk and the outer layer is wrapped with carbon shell [22]. The synergistic effect between them increases the rate performance and cycle stability of electrode materials. After 100 cycles at 2.0 A g^{-1} , the discharge capacity was 665 mA h g^{-1} and the capacity retention rate was 91.5%. Therefore, this paper will discuss the application of cobalt compounds, carbon nanomaterials, and their composites in lithium-ion batteries.

2.1. Co_3O_4

Currently, LIBs anode materials include the following categories: alloys [23,24], carbon-based materials [25,26], metal oxides [27,28], metal sulfides [29,30], and metal organic frameworks (MOFs) [31,32]. In addition, Manickam Minakshi et al. used binary transition metal oxides, phosphates, and molybdenum salts as anodes for LIBs and sodium-ion batteries (SIB) and achieved good experimental results [33–35]. The anode materials first explored for LIBs conversion reaction are first-row transition metal oxides (TMOs), such as Fe_2O_3 , MnO_2 , NiO , and Co_3O_4 [36,37], of which Co_3O_4 has the best performance [12].

In recent years, many scholars have studied it. For example, Dona Susan Baji et al. synthesized a new discoid Co_3O_4 with high porosity following a simple hydrothermal method [38]. The presence of porous structure and cavity in the structure will increase the surface area of Co_3O_4 , which can provide more locations and channels for the rapid diffusion of lithium-ions and adapt to the volume change during the charge and discharge process, resulting in a great increase in electrochemical activities. The material has a capacity of $510.5 \text{ mA h g}^{-1}$ after 50 charge and discharge cycles under 4.0 C conditions. Li et al. prepared 2D porous Co_3O_4 nanosheets by self-sacrificing template method. The two-dimensional porous structure promoted the diffusion of electrolyte and the inser-

tion/extraction of Li^+ during charge and discharge, thus enhancing its electrochemical performance [39]. After 100 cycles at a current density of 1 A g^{-1} , the discharge capacity of the material is still 1000 mA h g^{-1} , indicating that the material had a high discharge capacity and excellent cyclic stability. Zhang et al. synthesized hollow/porous Co_3O_4 nanospheres by a simple impregnation method using carbon spheres as sacrificial templates and a metal-organic skeleton (MOF) assisted strategy, and then annealed them in air [40]. The semicircle diameter of hollow/porous Co_3O_4 microspheres is much smaller than that of Co_3O_4 nanorods, indicating that the former has a lower contact impedance and charge transfer impedance as an anode material. The hollow porous Co_3O_4 microspheres provided a high reversible discharge specific capacity of about 550 mA h g^{-1} and showed excellent cycle stability and rate performance after 520 cycles at 100 mA g^{-1} current density. Li et al. successfully prepared ultrathin mesoporous Co_3O_4 by the calcination of precursor $\text{Co}^{\text{II}}\text{Co}^{\text{III}}$ -layered double hydroxide nanosheet arrays, which has an ordered sheet nanostructure and uniform mesoporous distribution [41]. The Co_3O_4 nanosheet arrays with medium thickness prepared by this structure have appropriate ultrathin thickness and abundant mesopores, showing their excellent electrochemical performance for LIBs. They have a high specific charge capacity of $2019.6 \text{ mA h g}^{-1}$ at the current density of 0.1 A g^{-1} , good rate performance, and significant cycle stability (There is still a high capacitance of $1576.9 \text{ mA h g}^{-1}$ after 80 cycles). This ultrathin nano-sheet structure makes lithium-ions have a larger specific area, shortens the transmission path of lithium-ions, and improves the storage performance of lithium-ions.

These results indicate that cobalt oxide as anode of lithium battery can improve its electrochemical performance by changing its morphology.

Controlling the synthesis temperature of cobalt oxide is the key to control its morphology. For example, the Co_3O_4 nanostructure presents a cubic shape and is composed of nanotubes [42]. The higher the synthesis temperature is, the faster the growth rate, and then the nanotubes are obtained. The Co_3O_4 nanostructured material has a high capacitance of 833 F g^{-1} . The material synthesized at the optimum temperature of $18 \text{ }^\circ\text{C}$ has high reversibility and can adsorb and desorb ions from aqueous solution.

However, when metal oxides are used as anode materials, their capacity decays rapidly, their intrinsic conductivity is relatively low, and they will have large volume changes in the processes of lithiation and delithiation, so their life cycle needs to be prolonged and their performance still needs to be further optimized, which limits their practical application in batteries [11].

2.2. Binary Metal Oxides

Binary metal oxide ACo_2O_4 ($A = \text{Ni, Fe, Mg, Zn, Mn}$) is a material obtained by partially replacing Co_3O_4 with other lower cost and environmentally friendly metals. The use of this material as the anode of lithium-ion batteries has been widely studied, and it is considered to have good development prospects [43–45].

For example, compared with the natural content of cobalt, manganese is more abundant, and the cost is 20 times lower than that of cobalt, which can effectively reduce the cost of anode materials. Badway and his colleagues coupled Co_3O_4 anode and LiCoO_2 cathode as a lithium-ion battery, which can provide a specific capacity of 120 mA h g^{-1} [46]. However, due to the high oxidation potential of Co, the average working potential of this cell is only 2.0 V. After introducing Mn into the A sites of the Co_3O_4 spinel structure, the actual working voltage of the battery can be increased by reducing the working voltage of the anode [12]. The synergistic effect of this bimetal also increases the theoretical capacity of the battery on the basis of Co_3O_4 [47–49].

When MnCo_2O_4 works as the anode active material of LIBs, it will inevitably produce volume change, which will affect the cycle performance of the battery [50–52]. Therefore, the researchers also explored the different morphologies [53–57] and composite structures of MnCo_2O_4 [58].

Islama et al. used the solvothermal method to prepare porous nanosheet-assembled MnCo_2O_4 microspheres as shown in Figure 2 [12]. The performance in practical applications is evaluated by testing the electrochemical response of the material in a cell structure. The energy density of the $\text{LiCoPO}_4/\text{MnCo}_2\text{O}_4$ cell reaches 415 W h kg^{-1} at high operating voltage [12].

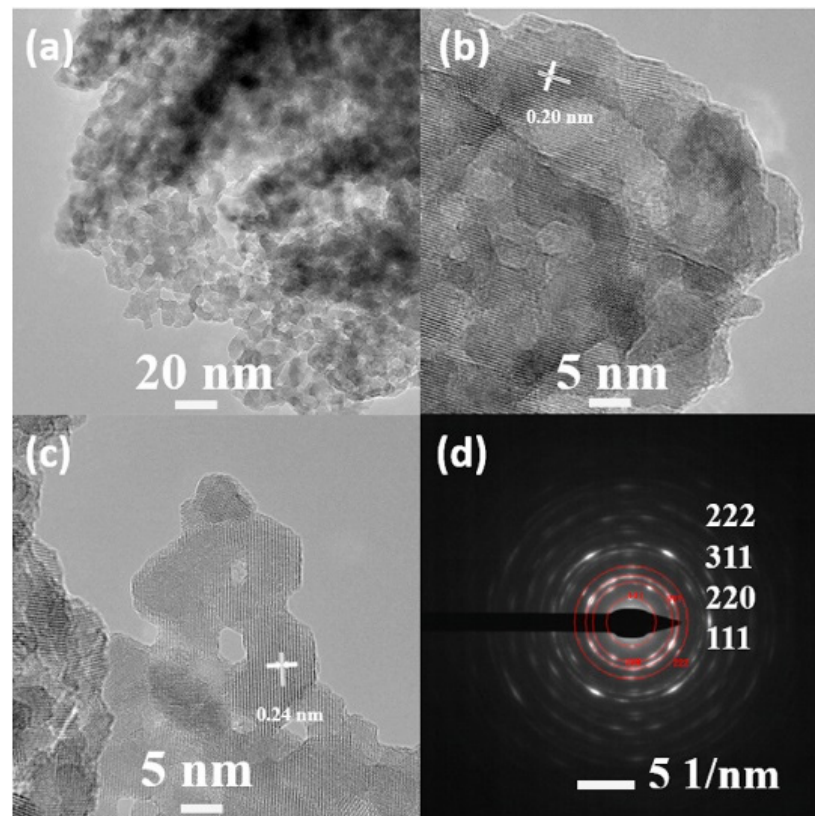
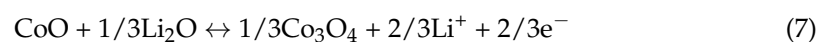
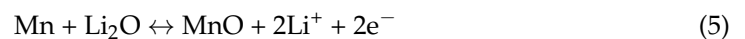


Figure 2. (a–d) TEM and HR-TEM images of a MnCo_2O_4 microsphere. Reproduced with permission from Mobinul Islam, A high voltage Li-ion full-cell battery with $\text{MnCo}_2\text{O}_4/\text{LiCoPO}_4$ electrodes; published by Elsevier, 2020 [12].

Xu et al. prepared three-dimensional porous hydrangea-like MnCo_2O_4 (h-MCO) by hydrothermal calcination [58]. As shown in the Figure 3, the micro morphology of MnCo_2O_4 is uniform rod, while hydrangea-like MnCo_2O_4 is spherical with roughly the same size. Zhang et al. used this three-dimensional porous h-MCO to obtain a lithium-ion battery [54]. The electrochemical reaction involved in the first discharge process of h- MnCo_2O_4 electrode can be expressed by the following equations [54,59,60]:



where Equation (4) represents the main reaction at the cathode, the decomposition of MnCo_2O_4 into Co and Mn and the production of Li_2O , which is accompanied by the growth of solid electrolyte interface (SEI) film. Equations (5)–(7) represent the main anodic reaction process, in which Mn and Co are oxidized to MnO and CoO, respectively, while Li_2O is decomposed to Li^+ and Co_3O_4 is produced.

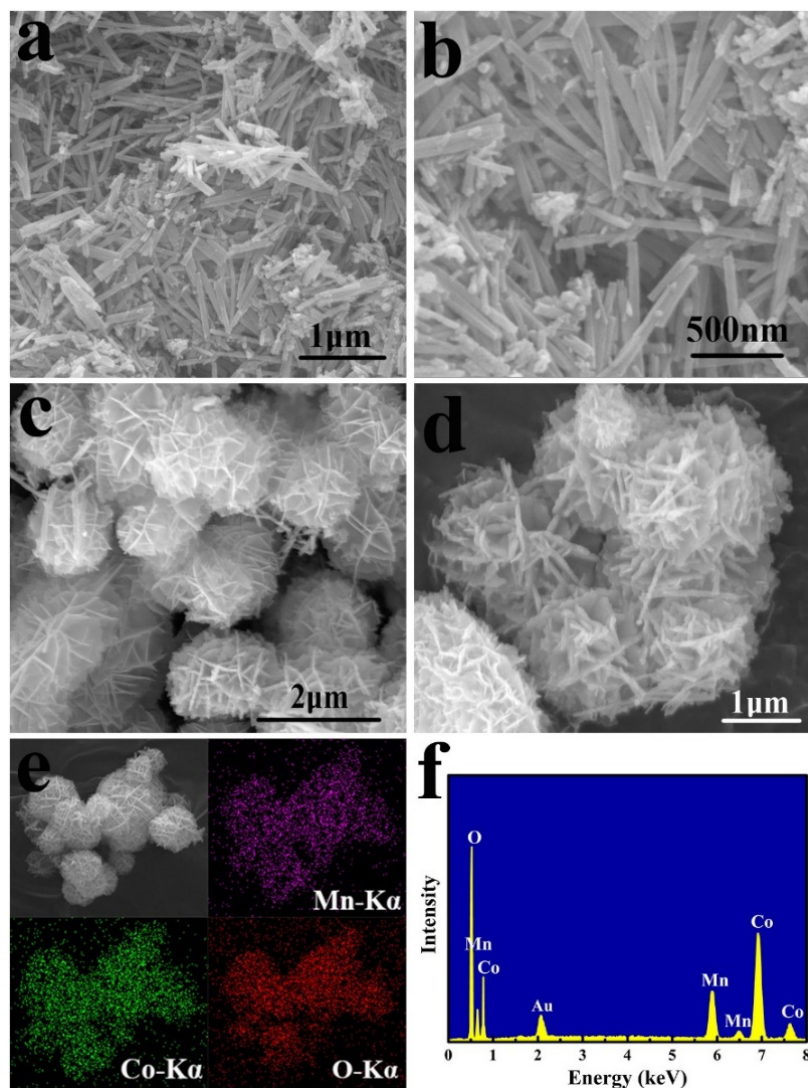


Figure 3. (a,b) The FE-SEM images of r-MCO; (c,d) The FE-SEM images of h-MCO; (e) The element mappings of h-MCO; (f) The EDS of h-MCO. Reproduced with permission from Xiaolan Song, Hydrothermal synthesis of porous hydrangea-like MnCo_2O_4 as anode materials for high performance lithium-ion batteries; published by Elsevier, 2019 [58].

In 100 cycles of 0.1 A g^{-1} , the reversible specific capacitance of h-MCO remains at 930 A h kg^{-1} and is higher than its theoretical capacity. As shown in Figure 4a, the reversible specific capacitance remains at 855 A h kg^{-1} in 300 cycles of 0.5 A g^{-1} and the reversible specific capacitance remains at 178 A h kg^{-1} in 600 cycles of 1 A g^{-1} . The specific capacity of h-MCO remains at 566 A h kg^{-1} even at a rate of 2 A g^{-1} . It can be seen that h-MCO has a good capacity retention rate. Figure 4b also shows that the cycle life of h-MCO electrode is longer than that of rod-shaped MnCo_2O_4 (r-MCO) electrode. Figure 4c shows that in a repetitive cycle, although the volume of the h-MCO electrode has been greatly expanded, it still retains its original hydrangea shape, indicating that it has a stable three-dimensional mesoporous hydrangea-like shape of spinel structure. The electrochemical impedance spectroscopy (EIS) of MCOs before and after cycling are determined, which shows that the h-MCO electrode had excellent electrochemical performance. Figure 4d shows that the conductive network and mesoporous structure developed by h-MCO can reduce the charge transfer resistance, and the ion diffusion resistance of the h-MCO electrode is small and the electron conductivity is better. This may be due to the larger

specific surface area of this material, the porous and rough surface, and its more stable three-dimensional structure [58].

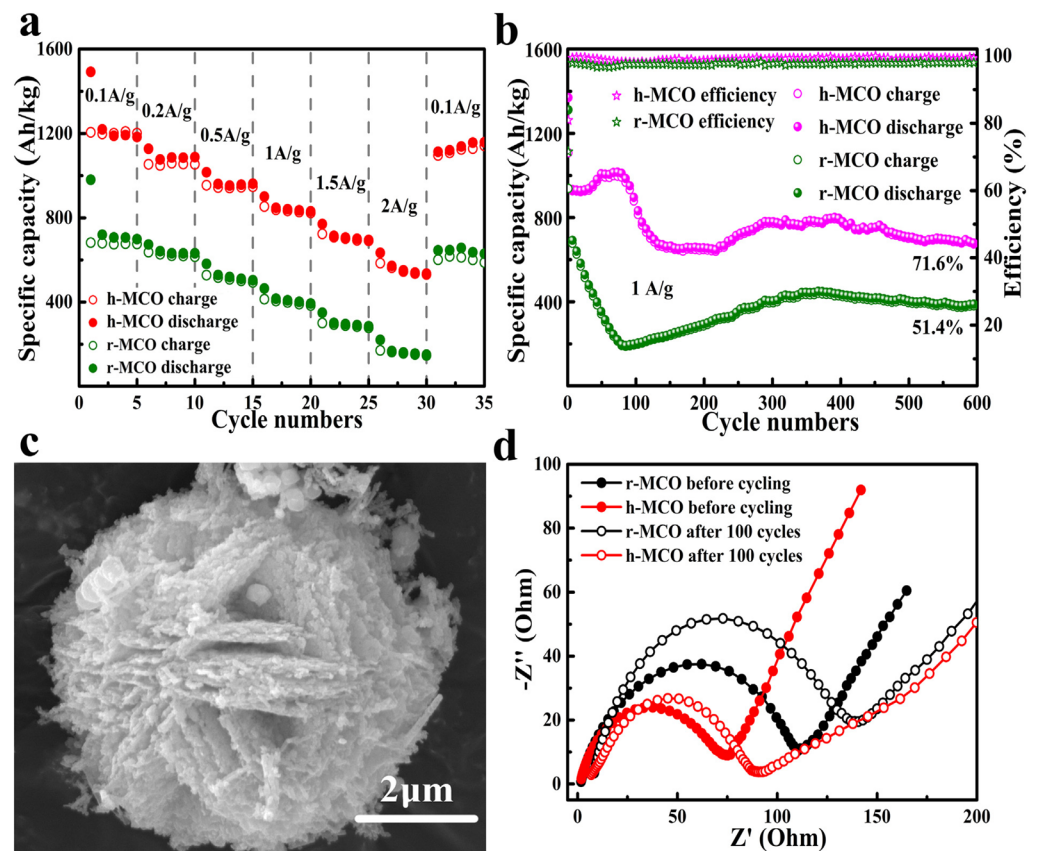


Figure 4. (a) Rate performances of the MCOs; (b) Long cycling performances of the MCOs at 1 A g^{-1} ; (c) FE-SEM image of h-MCO after 5 cycles at 0.1 A g^{-1} ; (d) Nyquist profiles of MCOs before cycling and after 100 cycles. Reproduced with permission from Xiaolan Song, Hydrothermal synthesis of porous hydrangea-like MnCo_2O_4 as anode materials for high performance lithium-ion batteries; published by Elsevier, 2019 [58].

In addition, there are many reports on MnCo_2O_4 materials with unique structures. As shown in Figure 5a,b, Jin's team [48] and Wu's team [61] produced MnCo_2O_4 mesoporous microspheres and verified their mesoporous structure respectively, and attributed the excellent electrical properties of the material to this mesoporous structure. Li et al. prepared MnCo_2O_4 sub-microspheres with different hollow structures of homogeneous MnCo_2O_4 sub-microspheres and verified that the yolk-shell structure (Figure 5c) had the best performance, because the mesoporous structure of the yolk-shell structure could improve the stability and thus the recyclability of the electrode. The hollow structure could expand the contact area between the electrode and the electrolyte and thus improve the specific capacity of the electrode [62]. Ding et al. similarly designed yolk-shell MnCo_2O_4 - TiO_2 sub-microspheres (Figure 5d), with the difference that MnCo_2O_4 acts as the core and TiO_2 constitutes the shell [51]. The porous yolk-shell structure slows down the volume change of the electrode material during the charging and discharging process and ensures a stable cycling performance. As in Figure 5e, Zhang et al. proposed a hierarchical self-assembled MnCo_2O_4 nanomembrane structure, and this material exhibited good cycling stability, especially at high current densities [54]. As shown in Figure 5f, Chen et al. embedded MnCo_2O_4 nanoparticles uniformly in paper-like graphene sheets, and the excellent conductivity of graphene films facilitated ion/electron transport during battery operation [50].

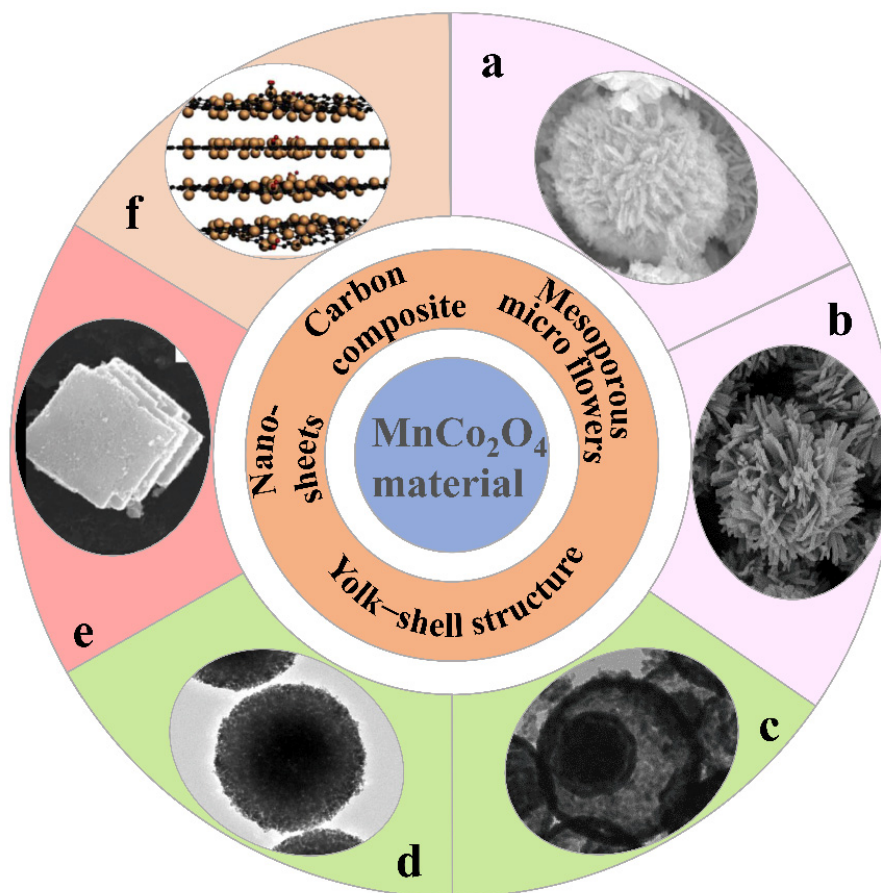


Figure 5. (a,b) Mesoporous micro flowers; Reprinted with permission from ref. [48]. Copyright 2016, Elsevier. Reprinted with permission from ref. [61]. Copyright 2015, Materials Letters. (c,d) Yolk-shell structure; Reprinted with permission from ref. [62]. Copyright 2013, ACS Applied Materials & Interfaces. Reprinted with permission from ref. [51]. Copyright 2017, Journal of Alloys and Compounds. (e) Nanosheets; Reprinted with permission from ref. [54]. Copyright 2015, Elsevier. (f) Carbon composite; Reprinted with permission from ref. [50]. Copyright 2016, Elsevier.

In conclusion, by controlling the morphology of MnCo_2O_4 material to form a mesoporous structure, the volume change resistance of microstructure can be improved, thus improving the cycle stability of electrode. By designing the hollow structure, the contact area between the electrode and electrolyte can be enlarged, and the specific capacitance of the electrode can be increased.

2.3. Application of Cobalt Oxide Composite

Studies have shown that by combining two or more transition metal oxides with other components, the resulting hybrid materials can combine the advantages of different substances to optimize the electrochemical performance of metal oxides [63,64].

$\text{Co}_3\text{O}_4/\text{CeO}_2$ is a material with high-rate capacity and high efficiency in Co_3O_4 matrix composites [65–68]. Kang et al. synthesized $5\text{Co}_3\text{O}_4/\text{CeO}_2$ ($\text{Co}_3\text{O}_4/\text{CeO}_2$ having the molar ratio of $\text{Co}/\text{Ce} = 5:1$) composites by the microwave-assisted solvothermal method (Figure 6). As shown in Figure 7, the micromorphology shows that the prepared sample is composed of irregular small pieces. The initial discharge capacity of $5\text{Co}_3\text{O}_4/\text{CeO}_2$ is $1090.1 \text{ mA h g}^{-1}$, and the reversible capacity is $1131.2 \text{ mA h g}^{-1}$ after 100 cycles at the current density of 100 mA h g^{-1} . The rate data indicate that the discharge capacity of $5\text{Co}_3\text{O}_4/\text{CeO}_2$ reaches $835.3 \text{ mA h g}^{-1}$ when the current density is 2000 mA g^{-1} . At the same time, the heterostructure of this material can also buffer the volume expansion and contraction of lithium-ion batteries during application [11].

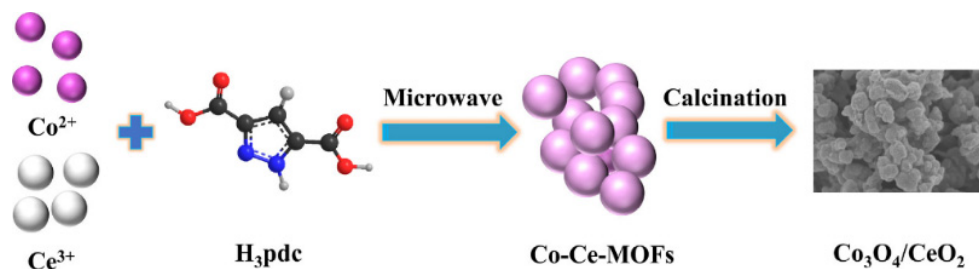


Figure 6. Schematic illustration of $\text{Co}_3\text{O}_4/\text{CeO}_2$ preparation. Reproduced with permission from Ying Kang, Highly efficient $\text{Co}_3\text{O}_4/\text{CeO}_2$ heterostructure as anode for lithium-ion batteries; published by Elsevier, 2020 [11].

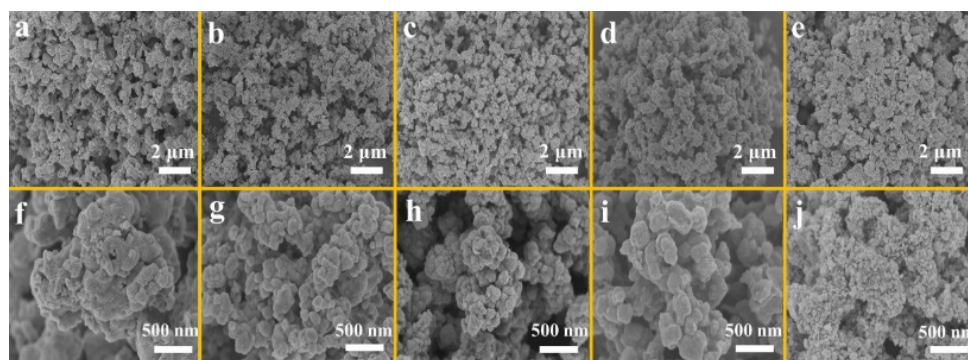


Figure 7. SEM images of (a,f) Co_3O_4 , (b,g) $\text{Co}_3\text{O}_4/\text{CeO}_2$, (c,h) $3\text{Co}_3\text{O}_4/\text{CeO}_2$ ($\text{Co}_3\text{O}_4/\text{CeO}_2$ having the molar ratio of $\text{Co}/\text{Ce} = 3:1$), (d,i) $5\text{Co}_3\text{O}_4/\text{CeO}_2$ ($\text{Co}_3\text{O}_4/\text{CeO}_2$ having the molar ratio of $\text{Co}/\text{Ce} = 5:1$), and (e,j) $7\text{Co}_3\text{O}_4/\text{CeO}_2$ ($\text{Co}_3\text{O}_4/\text{CeO}_2$ having the molar ratio of $\text{Co}/\text{Ce} = 7:1$). Reproduced with permission from Ying Kang, Highly efficient $\text{Co}_3\text{O}_4/\text{CeO}_2$ heterostructure as anode for lithium-ion batteries; published by Elsevier, 2020 [11].

Zhong et al. prepared $\text{Co}_3\text{O}_4\text{-CoFe}_2\text{O}_4$ nanocomposites by a one-step pyrolysis method. Such nanostructures are smaller in size and have a more uniform particle distribution, resulting in better electrochemical performance of the material [69]. Ding et al. synthesized $\text{Co}_3\text{O}_4@\text{TiO}_2$ hollow composites by using an imidazole zeolite framework-67 (ZIF-67) and thermal decomposition of the TiO_2 coating. When this material is used as an anode for LIBs, it shows a high cycle performance of 1057 mA h g^{-1} after 100 cycles at 100 mA g^{-1} [70].

2.4. Transition Metal Sulfide and Its Composites

In recent years, transition metal sulfides (TMS) have been gradually used as anode materials in lithium-ion batteries due to their large theoretical capacity, good redox potential, and low cost.

Similar to transition metal oxides, TMS electrodes also experience volume change during Li^+ insertion/extraction, which affects the cycling performance of Li-ion batteries [71]. The rational construction of nanostructured CoS_x can not only shorten the diffusion length of Li^+ ions and promote ion transport dynamics, but also provide buffer space for the volume change of CoS_x [72–74].

Yang et al. prepared a human spine-like CoMoS_3 nanostructure by a MOF-mediated approach, utilizing the synergistic effect of each component to enhance the electrochemical performance of the material [75]. Yu et al. synthesized NiCo_2S_4 nanotubes on the basis of nickel foam, which have excellent performance as anodes for LIBs [76].

By combining nanostructured transition metal sulfides with carbonaceous materials, the electrical conductivity can be improved, buffering the volume change, and thus prolonging the cycle life. For example, many researchers have prepared CoS_x/C nanocomposites by introducing carbon nanotubes, graphene, etc. [77–81].

Wang et al. fabricated a $\text{MoS}_2/\text{CoMo}_2\text{S}_4/\text{Co}_3\text{S}_4$ nanostructure supported by a graphene layer for use in the anode of LIBs [71]. The material has a rate performance of 360 mA h g^{-1} at 10 A g^{-1} and a specific capacity of 770 mA h g^{-1} at 0.2 A g^{-1} . As shown in Figure 8, they first obtained the ZIF-67 framework by precipitation, then coated the framework with molybdenum disulfide, and finally attached the sample to the surface of reduced graphene oxide and annealed it. CoMo_2S_4 is generated due to the interdiffusion of metal sulfides during annealing. $\text{MoS}_2/\text{CoMo}_2\text{S}_4/\text{Co}_3\text{S}_4$ nanostructures can improve surface area and facilitate ion transport. In addition, due to the presence of two-dimensional reduced graphene oxide, the conductive distance becomes longer, and the structure is more stable. Therefore, its rate performance, specific capacity, and stability all perform well.

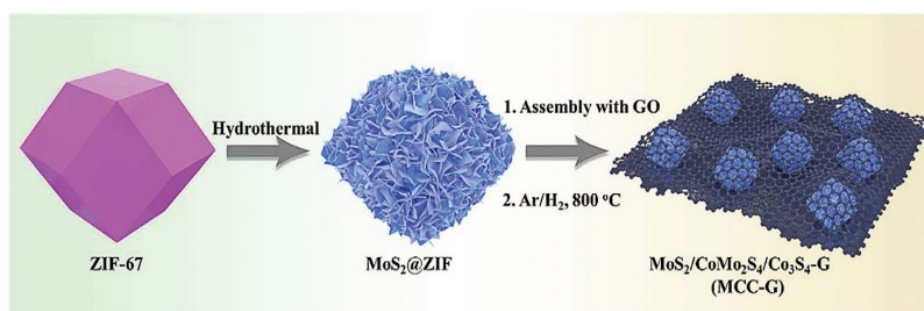


Figure 8. Schematic illustration for the fabrication of $\text{MoS}_2/\text{CoMo}_2\text{S}_4/\text{Co}_3\text{S}_4$ supported by graphene. Reproduced with permission from Pengcheng Wang, Constructing $\text{MoS}_2/\text{CoMo}_2\text{S}_4/\text{Co}_3\text{S}_4$ nanostructures supported by graphene layers as the anode for lithium-ion batteries; published by Royal Society of Chemistry, 2020 [71].

Zhu et al. prepared cobalt sulfide/reduced graphene oxide (CoS_x/RGO) nanocomposites by the hydrothermal method [82]. Comparing the micro morphology of CoS_x (Figure 9a) and the prepared CoS_x/RGO (Figure 9b), it is found that the aggregation of CoS_x particles is obviously more significant than that of CoS_x/RGO particles. This shows that CoS_x/RGO as a precursor can inhibit the agglomeration of CoS_x . As shown in Figure 10a, on the GCD curve of CoS_x/RGO , a long plateau at about 1.08 V can be observed in the first discharge curve, which is related to the intercalation reaction between Li^+ ions and CoS_x . Figure 10b shows that the discharge capacity of the composite at 50 cycles is 796 mA h g^{-1} . At a current density of 800 mA g^{-1} , CoS_x/RGO has a reversible capacity of 425 mA h g^{-1} (Figure 10c), which is higher than that of RGO and CoS_x , indicating that CoS_x/RGO has better rate performance than RGO and CoS_x . As shown in Figure 10d, through the EIS test (The equivalent circuit model is shown in the inset of Figure 10d), it can be seen that the combination of CoS_x and RGO reduces the charge transfer resistance of the electrode, thereby improving the lithium-ion storage performance.

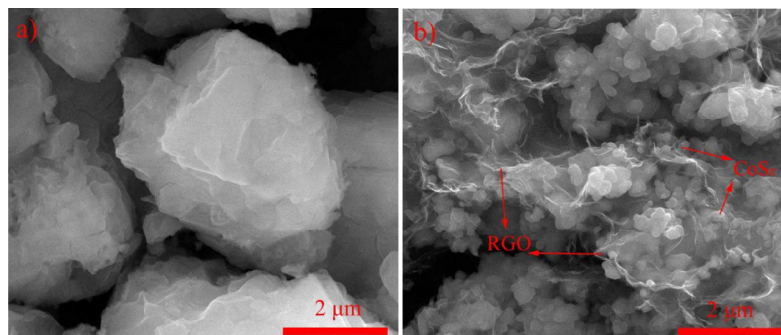


Figure 9. SEM images of (a) CoS_x ; (b) CoS_x/RGO . Reproduced with permission from Junsheng Zhu, Embedding cobalt sulfide in reduced graphene oxide for superior lithium-ion storage; published by Elsevier, 2019 [82].

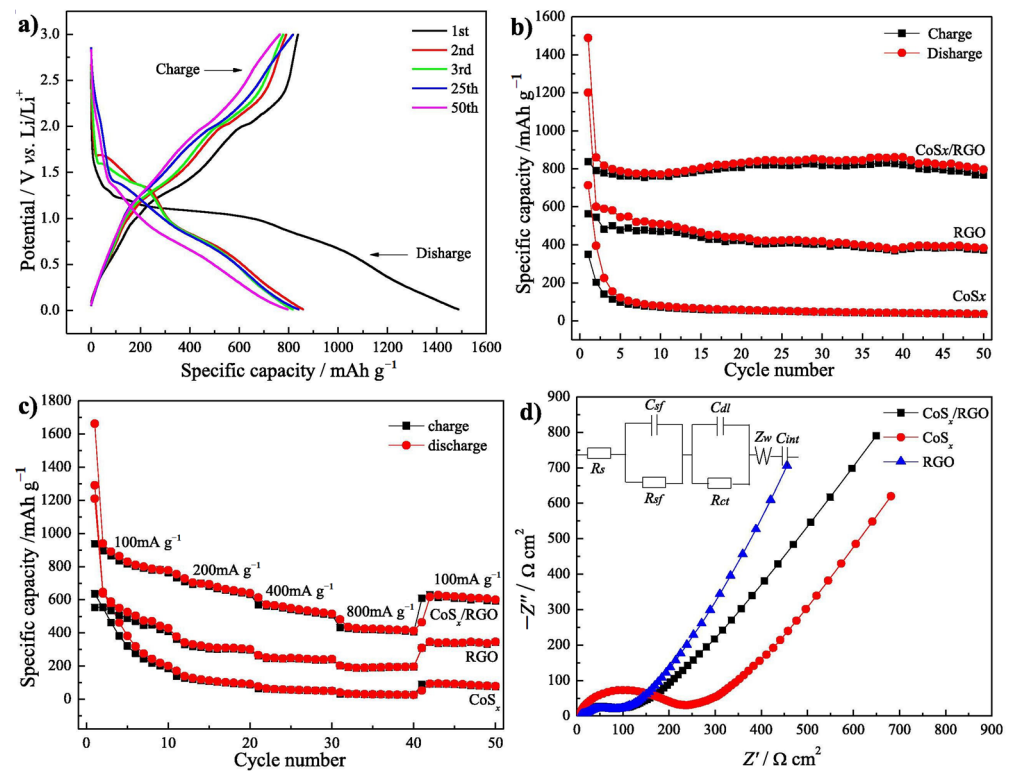


Figure 10. (a) GCD curves of CoS_x/RGO ; (b) Cycling performance of the samples; (c) Rate capability and (d) Nyquist plots of CoS_x , RGO and CoS_x/RGO . Reproduced with permission from Junsheng Zhu, Embedding cobalt sulfide in reduced graphene oxide for superior lithium-ion storage; published by Elsevier, 2019 [82].

In general, the construction of nanoelectrodes can shorten the Li^+ diffusion distance and boost the ion transport kinetics. Compared with single metal sulfides, multicomponent TMS not only have higher electrical conductivity, but also have more abundant redox reactions [71].

The rational design of nanostructured CoS_x can not only reduce the diffusion length of Li^+ ions, but also provide buffer space to accommodate the volume change of CoS_x [72–74]. Yu et al. constructed NiCo_2S_4 nanotubes on nickel foam, resulting in high-performance anodes of LIBs [76].

In addition, besides the above-mentioned cobalt-based materials, carbon-based materials with high chemical stability, strong conductivity, high specific surface area, and good capacity retention are also traditional anode materials in electrochemical energy storage devices [83,84]. Among them, graphite is the most widely used anode material in lithium-ion batteries. However, due to its low specific capacity (372 mA h g^{-1}) and slow lithium diffusion kinetics, its practical application is limited [85]. In the past 30 years, people have made great efforts to explore and develop new carbon materials with high capacity and good rate performance, such as carbon nanotubes [86,87], nanofibers [88,89], and graphene [90,91].

3. Application of Carbon Nanomaterials

3.1. Application of Carbon Nanotube Materials

Since carbon nanotubes (CNTs) were first observed in the process of carbon arc discharge in Iijima in 1991, there has been an upsurge in research concerning CNTs all over the world, and their basic properties and potential practical applications have become deeply understood. Structurally, CNTs are one-dimensional hollow cylinders with radial dimensions of nanometers and axial dimensions of microns, which are composed of one or more rolled graphene sheets. CNTs are one of the perfect anode materials for lithium

batteries because of their high conductivity, high chemical stability, and strong redox ability [92]. At present, a large number of studies have reported the successful use of CNTs as anodes of lithium-ion batteries. The results show that different morphologies, structures, and synthesis methods have great influence on the electrochemical properties of CNTs.

In previous research, the morphology and structure of CNTs were changed by ball milling or etching, and the reversible ability could be effectively improved. In the research of Yang et al., the electrochemical performance of multi-walled CNTs prepared by arc method can be effectively improved by etching, and the capacity retention rate of corroded CNTs are about 100% after 30 cycles [93]. In addition, electrochemical tests also show that the reversible capacity of the treated CNTs is four times that of the original CNTs. This remarkable improvement of reversibility can be attributed to the improvement of the purity of the original CNTs and the increase of active substances in the electrodes due to acid etching. At the same time, HRTEM images (Figure 11) show that the etched CNTs have new defects along the sidewalls, which are beneficial to the insertion and extraction of lithium-ions.

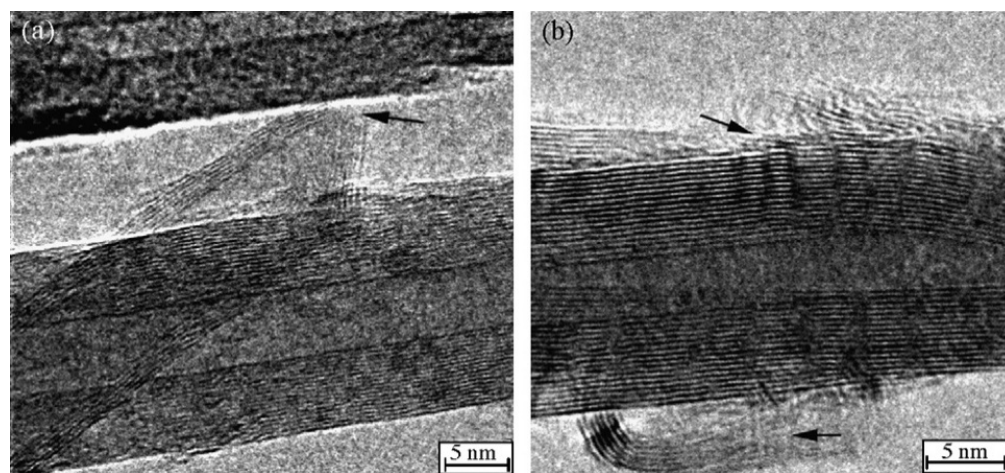


Figure 11. HRTEM images of etched CNTs. The black arrows in figures represent the etched position. Reproduced with permission from Shubin Yang, Electrochemical performance of arc-produced CNTs as anode material for lithium-ion batteries; published by Elsevier, 2007 [93].

Etching treatment effectively improves the recycling capacity of CNTs, while the irreversible capacity of CNTs after acid etching increases by 100 mA h g^{-1} compared with the original CNTs. This result is probably due to the formation of a large number of active functional groups which can promote electrolyte decomposition during acid corrosion and oxidation, and heat treatment can effectively alleviate this irreversible capacity increase. However, the defects produced by etching treatment are often accompanied by the decrease of Coulomb efficiency.

Besides etching, ball milling technology is also an important method to improve the electrochemical performance of CNTs. Eom et al. used stainless steel balls to ball-mill purified multi-walled CNTs in stainless steel bottles and dried them at $150 \text{ }^\circ\text{C}$ for 5 h [94]. The Coulomb efficiency of multi-walled CNTs increases with the increase of milling time by analyzing the charge-discharge characteristics of multi-walled CNTs. Their reversible capacity can reach 641 mA h g^{-1} , while that of pure multi-walled CNTs is only 351 mA h g^{-1} , and their irreversible capacity is reduced to about 1/2 of that of pure CNTs. The decrease of irreversible capacity is related to the increase of density of ball-milled multi-walled CNTs. For the increase of reversible capacity, Eom and others think that this is related to the fracture of a single carbon nanotube to form an open end and the formation of surface functional groups, which promotes the insertion of lithium-ions. Although ball milling can improve the reversibility and Coulomb efficiency of CNTs, the treated CNTs have a large voltage hysteresis problem, which Eom attributed to the formation of a large

number of active surface functional groups mentioned earlier. Gao et al. studied the ball milling treatment of single-walled CNTs, and thought that because single-walled CNTs are relatively defect-free materials, it is difficult to generate a large number of functional groups on the sidewalls, so their voltage hysteresis may be related to the kinetics of lithium diffusion to the inner core of CNTs [95]. Experiments show that the voltage hysteresis can be effectively alleviated by cutting CNTs into shorter tube segments, which has also been confirmed in the research of Yang et al. [96]. By analyzing the electrochemical performance of long and short CNTs, it is found that the reversible capacity of short carbon nanotube electrode reaches 266 and 170 mA h g⁻¹ at current densities of 0.2 and 0.8 mA cm⁻², respectively, which is almost twice that of long carbon nanotube electrode. Yang et al. think that the reason why long and short CNTs show this difference is related to the different lithium storage mechanism of their electrodes. For long CNTs, lithium-ions are mainly absorbed on one side of the graphene layer and combined with functional groups on the surface of CNTs, while short CNTs are mainly intercalated between graphene layers and doped into carbon nanotube microcavities. In addition, long CNTs have greater voltage hysteresis, which may be related to the surface functional groups and surface resistance of CNTs.

In addition to the above treatment of CNTs, the morphology of CNTs can be controlled by different synthesis methods, thus changing their electrochemical properties. Among them, Bulusheva et al. successfully synthesized and separated vertically arranged carbon nanotubes (VA-CNTs) on silicon substrate by meteorological assisted catalytic chemical vapor deposition method [97]. It is reported that VA-CNTs have better electrochemical performance than disordered carbon nanotube arrays. It is speculated that the reason for this may be that the vertically arranged structure increases the available surface area of electrolyte and lithium-ions, and then increases the specific capacity of CNTs.

Although CNTs have great application potential in the direction of anode materials for lithium-ion batteries, their application is limited due to their large structural defects and serious voltage hysteresis. In addition, compared with graphite, CNTs only demonstrate obvious improvement in capacity and cycle stability. Because their electrochemical performance is closely related to their structure and morphology, it is very important to control their structure and morphology in the preparation process, and the control of experimental conditions is also a crucial factor limiting their practical application.

3.2. Application of Graphene Materials

Graphene is a kind of material in which carbon atoms connected by sp² hybridization are closely packed into a single layer of two-dimensional honeycomb structure. Graphene has the same structural unit as the above CNTs [98], and has excellent conductivity and mechanical strength. At the same time, its specific surface area is as high as 2630 m² g⁻¹, and it has high thermal conductivity exceeding 3 × 10³ W m⁻¹ K⁻¹ [99–101]. Compared with CNTs, graphene may have lower treatment cost, higher purity, and more stable electrochemical performance, so the research on graphene in the field of energy storage has always been a hot spot in the international nanotechnology field [102–105]. The reversible capacity of the corroded CNTs are about four times that of the original CNTs (reversible capacity of 300–640 mA h g⁻¹). Their irreversible capacity (225 mA h g⁻¹) is higher than that of the original CNTs (125 mA h g⁻¹), and the capacity retention rate after 30 cycles is almost 100%. Graphene microspheres (453 mA h g⁻¹) have almost twice the specific capacity of multilayer graphene (MG, 229 mA h g⁻¹), and after 100 cycles the capacity is 94% of the original. Graphene nanosheets (GNSs), as anode materials for lithium-ion batteries, will have great application potential and are expected to replace CNTs [106]. In recent years, graphene paper, porous graphene nanosheets (PGNs), and graphene microspheres have also been reported as anode materials for lithium-ion batteries [107,108]. In Guo's research, GNSs with the disordered structure were successfully synthesized from artificial graphite by oxidation, rapid expansion, and ultrasonic treatment [109]. When the current density is 1 mA cm⁻², the reversible capacity of GNSs electrode is 554 mA h g⁻¹, which is

almost twice that of its raw material, artificial graphite. The results show that GNSs has higher reversible capacity, better cycle performance, and higher rates of charge-discharge performance than artificial graphite. This improvement in electrochemical performance can be attributed to the existence of more cavities or defects in GNSs which are beneficial to lithium storage and a large number of surface functional groups. In order to further improve the electrochemical properties of GNSs, the shape and structure of graphene nanosheets have become one of the important means. In one example, using copper nitrite as template and phenolic resin as a carbon source for the first time, PGNs with onion-like nano-pore junctions were successfully synthesized by graphitization at 2800 °C, which alleviated the problems of environmental protection in the preparation of traditional PGNs [110]. Different from the traditional graphene electrode, the PGNs have a relatively stable voltage platform at 0.01–0.2 V, and the specific capacity reaches 245 mA h g⁻¹. The onion-like porous structure increases the contact area between electrode and electrolyte, and this in turn increases the chance of lithium-ion insertion, facilitates the rapid charge-discharge process, and improves the diffusion rate, so that it has excellent high-speed performance.

Recently, Rish et al. successfully synthesized three-dimensional multilayer graphene nanostructures (3DMGs) by catalytic graphitization and chemical oxidation-thermal reduction with biomass-based activated carbon as precursor [111]. The synthesis process is shown in Figure 12.

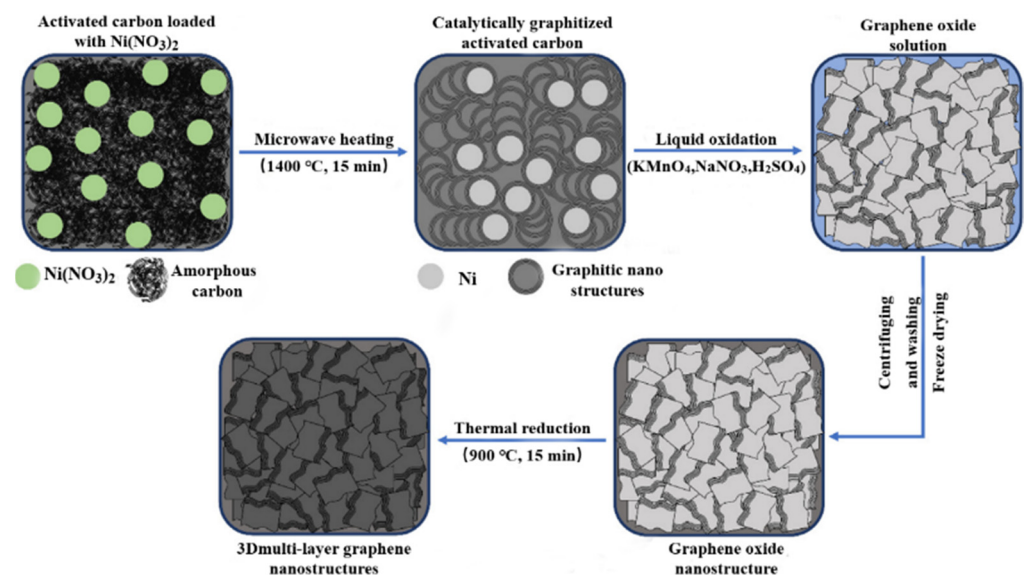


Figure 12. Schematic diagram of the synthesis process of 3DMGs. Reproduced with permission from SalmanKhoshk Rish, Novel composite nano-materials with 3D multilayer-graphene structures from biomass-based activated-carbon for ultrahigh Li-ion battery performance; published by Elsevier, 2021 [111].

As an anode material of the lithium-ion battery, the reversible capacity of synthesized 3DMGs can reach 1513.2 mA h g⁻¹ at 100 mA g⁻¹, second only to porous graphene, and the charge retention rate is 153.7%. After 1100 cycles at a high rate of 5000 mA g⁻¹, the specific capacity is 260.3 mA h g⁻¹, and the charge retention rate is 114.47%, which shows good cycle stability. This excellent electrochemical ability can be attributed to the interconnected pore structure and high specific surface area of 3DMGs. This unique structure provides more active sites and a shorter lithium-ion diffusion pathway for lithium-ion diffusion, which is convenient for rapid ion transport. In addition, the gap between nanostructures can be used as a buffer layer for volume expansion during the lithium-ion process, which can effectively prevent volume damage during charge and discharge and is conducive to improving its cycle stability. Compared with the traditional method of synthesizing

defective graphene, the above method uses green renewable carbon as precursor, and the preparation method is environmentally friendly, simple, and practical.

Compared with graphite, graphene has better electrochemical performance in lithium-ion battery anode materials. Because of its unique two-dimensional scalability, graphene can easily attach active material particles to the surface of other materials and is an excellent conductive carrier of battery materials. It is often polymerized with phosphate [112–115], silicate [116], and other polyanions as lithium-ion battery materials, showing more excellent electrochemical performance.

3.3. Application of Carbon Microspheres

In recent years, micron-sized carbon spheres (CSs) have been widely used in energy storage devices, such as LIBs [117], supercapacitors [118], lithium-sulfur batteries [119], and sodium ion batteries [120]. The research situation in recent years is shown in the Figure 13. Because of its high structural stability, high tap density, low surface volume ratio, and low viscous effect, it has great potential as anode material for LIBs [121–124]. In recent years, porous carbon materials have been studied as electrode materials. The micropores of carbon can effectively increase the specific surface area and enhance the contact between electrode and electrolyte. At the same time, the mesoporous structure can reduce the diffusion distance, thus improving the penetration and ion diffusion of electrolytes in carbon materials and realizing low resistance [125,126]. Therefore, nanoporous CSs have important research significance in the field of LIBs.

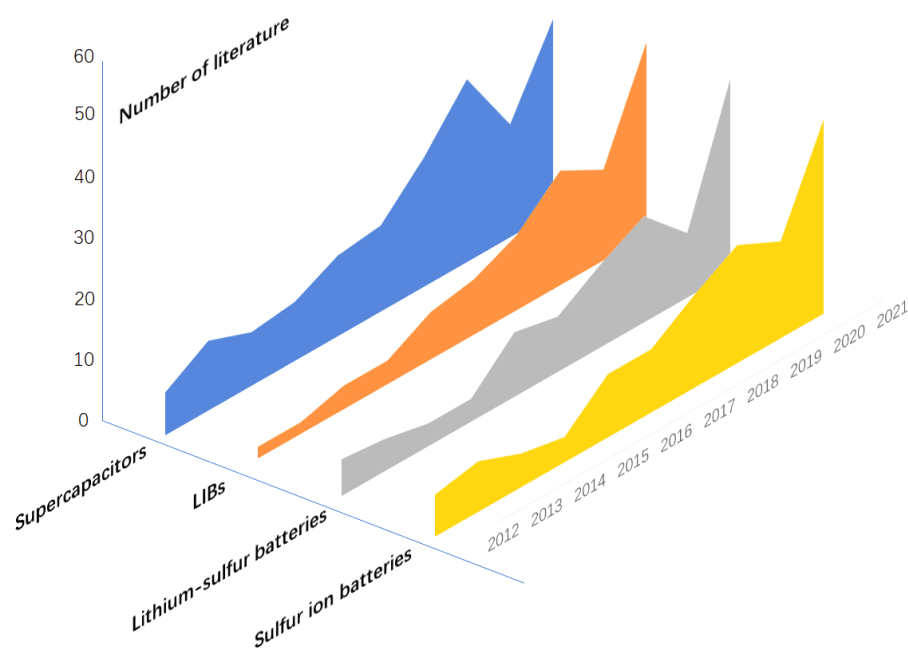


Figure 13. Research situation of CSs in LIBs, Lithium-sulfur batteries and Sulfur ion batteries from 2012 to 2021.

In Wang et al.'s research, layered porous carbon microspheres (HPCMs) with different surface morphology and internal structure were synthesized by alcohol emulsion technology with thermoplastic phenolic resin (PF) as carbon source and copper nitrate (CN) as template [127]. The results show that the content of copper nitrate can significantly affect the morphology and structure of samples, and then allow to prepare samples with different electrochemical properties. When the mass ratio of PF to CN is 1:4, the prepared HPCM not only keeps the structure of layered porous microspheres, but also has good electrochemical performance. At the current density of 50 mA g^{-1} , it has a reversible capacity of 585 mA h g^{-1} and remains at 480 mA h g^{-1} after 70 cycles.

In industrial production, the synthesis process of nano-porous carbon spheres usually needs pressurized containers and volatile organic compounds [128], which limits its large-scale application. Shi et al. successfully synthesized HPCMs with a loose porous structure by a simple impregnation-carbonization process with MgAl-layered double hydroxides precursor as template and MgAl-layered double oxides microspheres as carbon source [129]. The spherical structure effectively shortens the diffusion distance of lithium ions and provides higher tap density, while the existence of mesopores further shortens the diffusion channel. The results of electrochemical performance analysis show that when the template/carbon source mass ratio is 1, the capacities of the samples obtained at current densities of 0.05, 0.2, and 1 A g⁻¹ are 1140.5, 650.3, and 347.9 mA g⁻¹, respectively.

Although the porous structure increases the specific surface area, its initial Coulomb efficiency is low because of the larger surface area and more active sites in direct contact with electrolyte. Therefore, how to avoid the porous structure facing electrolyte directly becomes the key to solve this problem. At the same time, the materials with pure porous structure have poor mechanical properties, which leads to poor cycle performance when they are used as electrode materials. Zhang et al. synthesized bivalve pomegranate-like porous carbon microspheres (PCMs) considering this problem [130]. The porous carbon frame is wrapped by a carbon coating on its surface. The microscopic image shows that the outer carbon coating has a multilayer structure, an interconnected porous network structure is formed inside, and the hollow carbon spheres are connected with each other.

This double carbon shell structure can limit the formation of most solid electrolyte membranes to the outer surface, effectively prevent electrolytes from entering the inner surface, improve its conductivity, and enhance its mechanical properties. In addition, the interconnected porous carbon framework can provide more positions for lithium ion insertion, shorten the diffusion distance between electrons and ions, and promote the transfer of lithium ions and electrolyte diffusion. Through the analysis of electrochemical test results, PCMs show an initial Coulomb efficiency of over 91%, which is much higher than other porous carbon anode materials (less than 70%). In addition, PCMs have capacity of 580 and 520 mA h g⁻¹ at current densities of 1000 and 2000 mA g⁻¹, respectively. The synthetic method can effectively enhance its mechanical properties by introducing carbon coating, and at the same time prevent electrolytes from entering, which effectively improves the shortcomings of poor mechanical properties and low initial Coulomb efficiency of porous nano-carbon materials.

Recently, Zhang and his colleagues efficiently converted biomass carbon into high value-added graphite by electrochemical graphitization of glucose carbon [131]. Glucose was first converted into amorphous nanospheres or microspheres carbon. Then, the amorphous carbon was graphitized electrochemically in molten calcium chloride, and the hollow microspheres graphite with nano-flake porous shell were successfully prepared. The morphology evolution of graphite was analyzed by SEM and TEM. When the amorphous microspheres carbon (AMC) was simply immersed in the 820 °C melt for 2 h (without cathodic polarization), it can be seen that amorphous carbon microspheres have no morphological change (Figure 14b). After polarization at 0.45 V for 0.25 h, some protrusions appear on the surface of carbon microspheres (Figure 14c), and AMC spheres transform into porous structures composed of nano-sheets after polarization for 2 h (Figure 14d). It can be observed from Figure 14e,f that the original amorphous carbon spheres are dense while the graphitized carbon spheres are hollow. This unique hollow and porous shell structure provides more electrolyte channels and accelerates ion transmission in the electrode. When it is used as the anode material of a lithium-ion battery, it can provide a reversible capacity of about 280 mA h g⁻¹ at the charge and discharge rate of 5 C (1.86 A g⁻¹). Zhang put forward the corresponding concept of “electrochemical graphitization” in research that found that cathodic polarization in molten chloride can graphitize amorphous carbon at about 820 °C, and this method has been proved to be suitable for all amorphous carbon, providing a basis for preparing sustainable graphite as a high-performance anode [132–138].

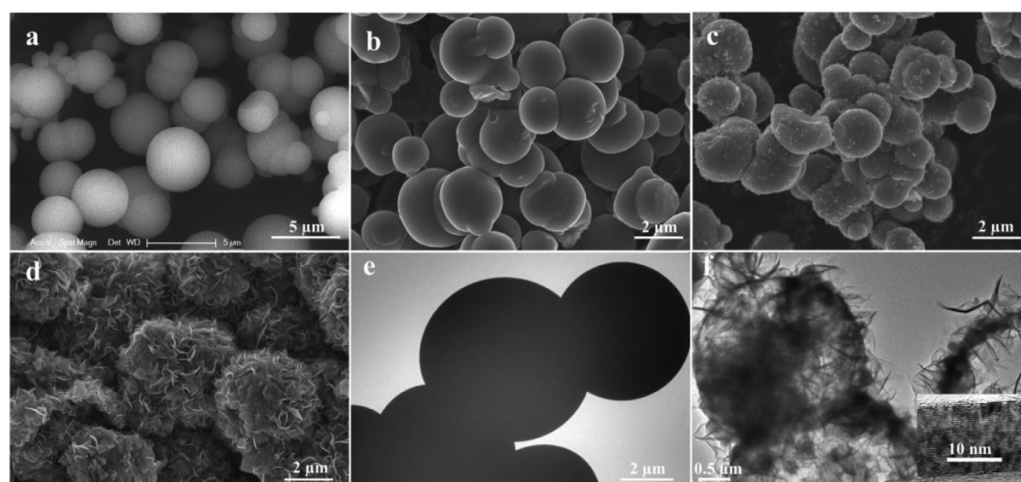


Figure 14. (a–d) SEM images of AMC before (a,b) And after (c,d) The electrochemical graphitization at 820 °C. (a) Raw; (b) Immersed in the melt for 2 h; (c) 0.45 V for 0.25 h; (d) 0.45 V for 2 h; (e,f) TEM images of AMC; (e) And the graphitized AMC at 820 °C and 0.45 V for 2 h. Reproduced with permission from Chunyan Zhang, Glucose-derived hollow microsphere graphite with a nanosheets-constructed porous shell for improved lithium storage; published by Elsevier, 2021 [131].

To sum up, carbon nanotubes, graphene and carbon microspheres have great application potential in lithium-ion batteries, but they also have certain advantages and disadvantages. Therefore, we made a simple comparison of the electrochemical properties of the three (Table 1).

Table 1. Comparison of electrochemical properties of carbon microspheres, graphene and carbon nanotubes.

Types of Materials	Cycle Number	Current Density	Reversible Capacity (mA h g ⁻¹)	Structure	Reference
Nanoporous carbon microspheres	500	200 mA g ⁻¹	650	double-carbon-shell	[130]
NCMs	50	210 mA g ⁻¹	926.654	porous spherical	[121]
AMC	100	1860 mA g ⁻¹	280	hollow microsphere	[131]
GNSs	30	0.2 mA cm ⁻²	502	disordered graphene layers	[109]
N-GNSs	100	100 mA g ⁻¹	760	porous architecture	[139]
Porous graphene film	50	50 mA g ⁻¹	195	porous structure	[140]
3DMGS	170	100 mA g ⁻¹	1513.2	multilayer nanostructures	[111]
CNTs	30	0.2 mA cm ⁻²	266	single-walled	[96]
VA-CNTs	50	100 mA g ⁻¹	350	multi-walled	[97]

As shown in Table 1, carbon nanomaterials with different morphologies show different electrochemical properties, and the influence of Co₃O₄ morphology on properties and control methods are also mentioned in the previous article, so controlling the morphology of carbon nanomaterials is also an extremely important method to improve electrochemical properties. In the research of Sun-Hwa Yeon et al., the morphology of graphene was successfully changed by ultrasonic treatment [141]. After ultrasonic treatment, the central folds of graphene flatten and transform into a honeycomb lattice, and the thickness of lamellae is relatively thinner. After 50 cycles at the same current density, the capacity retention of graphene before treatment is only 74%, while that of graphene nanosheets after treatment is 93%, which obviously improves the cycle performance. In addition, Sun et al. proposed to transform graphene oxide into graphene aerogel (GA) with porous three-dimensional structure by a simple hydrothermal method and freeze-drying process [142]. At the same time, it is found that the surface defects of GA can be regulated by controlling

the reaction time, and the formation of these surface defects can increase the active sites. In addition, by observing the micro-morphology of graphene nanosheets, it is found that the porous structures in graphene nanosheets form an interconnected network structure. A porous structure increases the contact area between electrolyte and electrode, which can effectively transfer electrons and ions into electrodes. At the same time, the formation of defects also greatly improves the electrochemical stability and rate performance of electrodes. In addition, Lee et al. controlled the morphology of three-dimensional CNTs grown on Cu by changing the temperature [142]. The results show that the average diameter of CNTs grown at high temperature (750 °C) is 200–300 nm, while the diameter of CNTs grown at low temperature (700 °C) is only about 20 nm. Among them, the performance of short diameter CNTs is obviously better than that of long diameter CNTs, which is largely related to the diffusion distance of lithium ions. The diameter is short and the diffusion distance is short, so the lithium ion diffuses rapidly. The above results show that the electrochemical performance of the materials can be improved by changing the morphology of the materials under the control of the experimental conditions.

4. Application of Cobalt-Carbon Composites

As mentioned earlier, cobalt and carbon materials have great application potential in lithium-ion battery anodes, and compounding various materials is also the main method to improve the electrochemical performance of cobalt nanomaterials. Among them, carbonaceous materials have become one of the ideal materials for composites with cobalt nanomaterials because of their high conductivity, and they have attracted wide attention in recent years. Among these materials, the more common one is to composite nano cobalt oxide and cobalt sulfide with carbonaceous materials.

4.1. Cobalt Oxide-Carbon Composites

As previously mentioned, pure Co_3O_4 with high theoretical capacity of 890 mA h g^{-1} has great application potential in the anode field of lithium-ion batteries. However, its low conductivity and large volume change during the lithiation and delithiation process leads to poor cycle performance and rate ability, which limits its commercial application. Researchers have tried to mitigate the influence of large volume changes through a large number of studies, including reducing the size of Co_3O_4 particles to nanoscale [143,144], morphological specialization [145,146], and combining with carbon materials [147,148] or metal oxides. Among these methods, the combination of Co_3O_4 and carbon material is the most promising, because carbon coating not only buffers the volume change, but also promotes the electronic conductivity. A large number of researchers have introduced different carbonaceous materials, including graphene [149–151], porous carbon [152], and carbon nanotubes [153,154], to improve their electrical conductivity.

Yan et al. synthesized carbon-doped Co_3O_4 hollow nanomaterials by an electrospinning and hydrothermal method with electrospinning as the template and carbon source for the first time [155]. The doping of carbon can reduce part of Co^{3+} to Co^{2+} , which provides more Co^{2+} and produces oxygen vacancies. Co^{2+} has higher electronegativity, which improves the capacity and enhances the rate capability of materials. At the same time, the introduction of oxygen vacancies and the hollow structure of the material shorten the Li^+ diffusion path and provide enough voids to accommodate the volume change. In addition, density functional theory (DFT) calculation further explains the conductivity enhancement of C-doped Co_3O_4 hollow nanofibers, which is related to the delocalization of its larger energy band structure, and further proves that this method can be used to prepare other transition metal oxide anodes. Compared with undoped Co_3O_4 hollow nanofibers (initial discharge and charge capacity of 1230 and 849 mA h g^{-1} , respectively, the initial discharge and charge capacity of C-doped Co_3O_4 increased to 1385 and 972 mA h g^{-1} . At the same time, after 100 charge-discharge cycles, the reversible capacity of carbon-doped Co_3O_4 remained at 1121 mA h g^{-1} , which was higher than that of undoped Co_3O_4 (663 mA h g^{-1}). Although the electrochemical properties of Co_3O_4 hollow nanofibers have been improved

after doping with carbon, with the continuous exploration of scholars in recent years, some other doping methods have appeared, one after another. For example, in 2015, Wang et al. successfully controlled the diameter of Co_3O_4 particles to about 5 nm, and synthesized a Co_3O_4 -carbon nanosheet structure in which nano- Co_3O_4 was anchored in the three-dimensional array of carbon nanosheets [156]. When used as anode material for lithium-ion batteries, its reversible specific volume can exceed 1200 mA h g^{-1} . Yang and his colleagues successfully prepared Co_3O_4 /onion-like carbon (OLC) nanocomposites with high area by a simple solvent method [157]. Nanoparticles of onion carbon composed of quasi-spherical graphite shell have isotropic surface, and lithium-ions can pass through electrolyte from all directions, which increases the conduction rate of lithium-ions. When used as anode material, the specific capacity was kept at 632 mA h g^{-1} after 100 cycles at the current density of 200 mA h g^{-1} , and the anode material showed good electrochemical performance, in which the onion-like structure played an important role. Similarly, Wang et al. successfully synthesized Co_3O_4 /carbon ($\text{Co}_3\text{O}_4/\text{C}$) materials with onion-like structure by carbothermal reduction and low-temperature oxidation with $(\text{BMIM})\text{N}(\text{CN})_2$ as precursor, in which Co_3O_4 was embedded in carbon matrix and showed good performance as anode material for lithium-ion batteries [158].

In addition, the introduction of porous carbon into Co_3O_4 also shows good effect. In the research of Han et al., Co_3O_4 nanoparticles (NPs) were uniformly immobilized on porous carbon (PC) by solvothermal method and simple heat treatment process, and cobalt oxide modified porous carbon was prepared [159]. The three-dimensional layered porous structure of the composites and the small size of Co_3O_4 NPs promote the diffusion of electrolytes and the insertion of lithium ions. Moreover, the interconnection network of porous carbon not only reduces the internal resistance of lithium-ion batteries, but also provides a mechanical buffer to prevent large volume changes, which plays a role in maintaining structural stability. When used as anode material for lithium-ion batteries, the composite material shows excellent cycle performance, high conductivity, and good rate performance. $\text{Co}_3\text{O}_4/\text{PC}$ composites can make full use of the advantages of Co_3O_4 and hierarchical porous carbons and show reversible properties of 654 mA h g^{-1} . It is proven that the composite of porous carbon materials and cobalt oxide materials is an effective method to improve the electrochemical properties of single cobalt oxide materials. In addition, the effectiveness of this method is also verified in the research of cobalt oxide compounding with porous carbon materials derived from carbon dioxide [19]. The synthesized cobalt oxide/porous carbon composites have a reversible capacity of 1179 mA h g^{-1} (higher than $\text{Co}_3\text{O}_4/\text{PC}$), and the reversible capacity remains at 1179 mA h g^{-1} after 300 cycles at 1000 mA g^{-1} .

Gu et al. prepared a new type of active porous carbon (APC) with lotus-like layered porous structure, and fixed cobalt oxide nanoparticles on the surface and pores of APC, to successfully prepare $\text{Co}_3\text{O}_4/\text{APC}$ nanocomposites [20]. APC, which has a large number of mesoporous and microporous structures, provides more active sites for the loading of nano- Co_3O_4 particles, reduces the agglomeration of Co_3O_4 particles on the surface, and can effectively alleviate the volume expansion effect. When the composite material is used as anode material for the lithium-ion battery, the reversible capacity is 625 mA h g^{-1} after 200 cycles at the current density of 500 mA g^{-1} , which is better than pure Co_3O_4 and $\text{Co}_3\text{O}_4/\text{PC}$ composites. In addition, the displayed discharge capacity at a current density of 1000 mA g^{-1} is about 360 mA g^{-1} , and the reversible capacity becomes 810 mA g^{-1} when the current density drops to 100 mA g^{-1} again. Among them, APC is prepared by activation and carbonization with waste loose manure as carbon source. The synthesis method is simple, the raw material cost is low, and it can be prepared in large quantities, which provides a new method for the preparation of cobalt oxide-carbon nanocomposites.

To sum up, the composite of carbon and Co_3O_4 nanomaterials plays a better role in improving the electrochemical properties of Co_3O_4 materials and has become one of the main methods to improve the electrochemical properties of Co_3O_4 materials, which has been studied more. Comparatively speaking, carbon materials with porous structure have

a stronger effect on enhancing the electrochemical performance of Co_3O_4 materials than ordinary carbon materials, which is related to its porous structure. In future research, we can further explore ways to improve the contact area between electrodes and electrolytes and increase the number of holes.

4.2. Co Sulfide-Carbon Composite in LIBs Anode

It has been proven that cobalt sulfide has better electrochemical performance than cobalt oxide, and the introduction of carbon nanomaterials into cobalt oxide has a very good effect. Therefore, researchers have also explored many methods to introduce carbon nanomaterials into cobalt sulfide and achieved good results.

Similar to cobalt oxide mentioned earlier, porous carbon materials have attracted more attention in the composite research of cobalt sulfide and carbon nanomaterials. The cobalt sulfide nanocomposite with porous carbon fiber intercalated ($\text{Co}_9\text{S}_8@\text{C}$), prepared by simple carbonization and sulfurization steps, shows good performance as an anode material for lithium ion batteries, which proves that the composite of porous carbon and cobalt sulfide is a method to improve its electrochemical performance [160]. The porous structure of carbon and the mesoporous structure of Co_9S_8 enlarge the interface between electrode and electrolyte, promote the transport of lithium ions, and prevent the aggregation and volume change of Co_9S_8 particles, thus improving the electrochemical performance. Its reversible capacity can reach 1565 mA h g^{-1} at 0.1 C rate. In the aspect of cycle stability, after 100 cycles, the specific discharge capacity remained at 872 mA h g^{-1} (Co_9S_8 was 294 mA h g^{-1}), while after 300 cycles, it still had a reversible capacity of about 606 mA h g^{-1} . Huang and his colleagues prepared polycrystalline Co_9S_8 coated with porous carbon [161]. Because of its porous structure and carbon coating, it shows excellent electrochemical performance as an anode material for lithium-ion batteries. After 400 cycles at 2 A g^{-1} , the capacity retention rate is 84.7%, and it has great prospects as a LIB anode material.

In addition, the composite of carbon nanosheets, carbon nanotubes, and cobalt sulfide also shows good results and has been studied by a large number of scholars. In the research of Shi et al., cobalt sulfide/carbon composites were prepared from metal-organic framework, and the flaky three-dimensional hollow cobalt sulfide/carbon nanosheet array ($\text{h-Co}_4\text{S}_3/\text{CNA}@\text{CC}$) grown on carbon cloth has good rate ability and cycle stability when used as anode of lithium-ion battery [162]. Among them, Co_4S_3 is wrapped in graphite carbon cage like pomegranate, and this unique structure can effectively buffer the volume expansion in physical and chemical process. In addition, carbon cloth is used as the substrate, which provides a large number of active sites and avoids the use of additives. As the anode of a lithium-ion battery, it has $654.3 \text{ mA h g}^{-1}$ and $394.1 \text{ mA h g}^{-1}$ at current densities of 1 A g^{-1} and 2 A g^{-1} , respectively. After 500 cycles at a current density of 2 A g^{-1} , the capacity retention rate reaches 79%.

In addition, Wang et al. successfully synthesized layered CoS_{1-x} nanoparticles/porous carbon nanoparticles ($\text{CoS}_{1-x}@\text{PCSs}$) by annealing and vulcanization with $\text{Co}(\text{OH})_2$ nanoparticles and sodium citrate as precursors. $\text{CoS}_{1-x}@\text{PCSs}$ composites have a large number of active sites and abundant nano-pores on the surface of carbon sheets, which can effectively improve the ion/electron transfer efficiency [163]. At the same time, the thin carbon structure encapsulates CoS_{1-x} nanoparticles, which can prevent cobalt sulfide from aggregating in the electrochemical process, buffer the volume change, isolate active substances and electrolytes, and improve the conductivity. The synergistic effect between the cobalt sulfide and carbon coating makes $\text{CoS}_{1-x}@\text{PCSs}$ composites have excellent lithium storage performance. As an anode of lithium-ion battery, it has a reversible capacity of $1199.6 \text{ mA h g}^{-1}$ after 100 cycles at 0.1 A g^{-1} , and a capacity of $825.7 \text{ mA h g}^{-1}$ after 800 cycles at a current density of 1 A g^{-1} . In addition, in the research of Wu and his colleagues, a porous carbon polyhedron/carbon nanotube hybrid was combined with cobalt sulfide material to synthesize three-dimensional hollow cobalt sulfide@porous carbon polyhedron/carbon nanotube hybrid ($\text{CoS}_{1-x}@\text{PCP}/\text{CNTs}$) material [164]. As shown in Figure 15a,b, the product obtained at $600 \text{ }^\circ\text{C}$ has a discharge capacity of 1668 mA h g^{-1} at a current density of 0.2 A g^{-1}

after 100 cycles, and its cycle performance is excellent, which is higher than that of the product obtained at 500 and 700 °C. With its excellent cycle performance, its charge and discharge capacities in the first cycle at 0.2 A g⁻¹ are 1246 and 2083 mA h g⁻¹, respectively, with an irreversible capacity loss of about 40%.

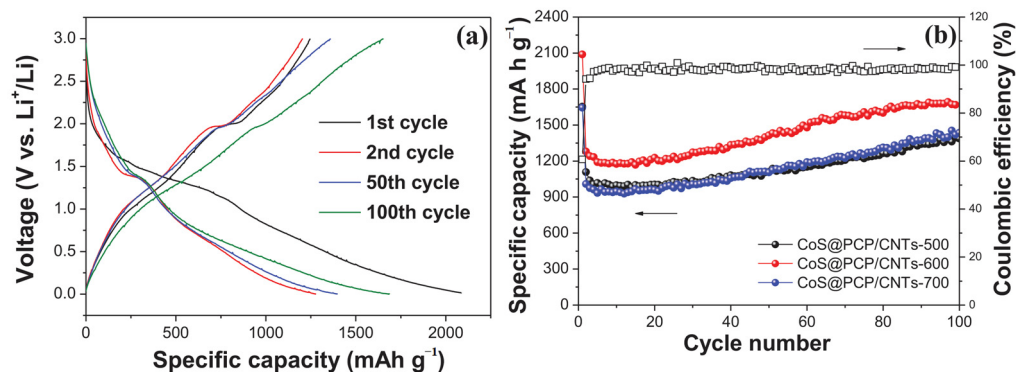


Figure 15. (a) Galvanostatic charge-discharge voltage profiles of 3D hollow CoS@PCP/CNTs-600 polyhedral at the current density of 0.2 A g⁻¹; (b) Cycling performances of CoS@PCP/CNTs-500, CoS@PCP/CNTs-600, and CoS@PCP/CNTs-700 and Coulombic efficiency of CoS@PCP/CNTs-600 at the current density of 0.2 A g⁻¹. Reproduced with permission from Wu, In-Situ Formation of Hollow Hybrids Composed of Cobalt Sulfides Embedded within Porous Carbon Polyhedra/Carbon Nanotubes for High-Performance Lithium-Ion Batteries; published by Advanced Materials, 2015 [164].

As shown in Table 2, cobalt-carbon composite nanomaterials show excellent electrochemical performance compared with cobalt compounds and carbon nanomaterials alone. To sum up, combining cobalt-containing nanomaterials with carbon nanomaterials and controlling the micro-morphology of the composites (such as improving the porosity of the materials and constructing porous network structure, etc.) to make them have a larger contact area with electrolytes is an effective method to improve the electrochemical performance of materials, which has great application potential in the field of anode materials for lithium-ion batteries.

Table 2. Comparison of electrochemical properties of cobalt compounds, carbon nanomaterials and cobalt-carbon composites.

Types of Materials	Current Density (A g ⁻¹)	Structure	Cycle Number	Reversible Capacity (mA h g ⁻¹)	Reference
Co ₃ O ₄	1.8 (2C)	porous disk-like	100	304	[165]
Ultrathin mesoporous Co ₃ O ₄ nanosheet	2	irregular small blocks	50	479	[166]
Co ₃ O ₄	0.4	porous microspheres	40	654	[167]
Co ₃ O ₄	0.8	mesoporous microstructure	50	260	[168]
Co ₃ O ₄	2	porous nanorod	25	516	[169]
Co ₃ O ₄	2	nanocages	25	252	[38]
Co ₃ O ₄ microspheres	0.1	hollow and porous	520	550	[40]
Co ₃ O ₄ Nanosheet Arrays	0.1	mesoporous	80	1576.9	[41]
CoS ₂	0.1	hollow spheres	40	320	[170]
2D Co ₃ S ₄	0.7	nano thickness sheet-like	400	416	[171]
MnCo ₂ O ₄	0.4	core-shell ellipsoidal	150	620.0	[53]
MnCo ₂ O ₄	0.1	nano sheet	50	681	[54]
MnCo ₂ O ₄	1	hierarchical porous	1000	740	[53]
CoMn ₂ O ₄	1	microspheres	1000	420	[57]

Table 2. Cont.

Types of Materials	Current Density (A g ⁻¹)	Structure	Cycle Number	Reversible Capacity (mA h g ⁻¹)	Reference
MnCo ₂ O ₄	0.1	porous hydrangea-like	100	930	[58]
Co ₉ S ₈	2	hollow nanospheres of mesoporous	800	896	[73]
Nitrogen-Doped Carbon Nanosheets	1	porous nanosheets	1000	222	[172]
Carbon	0.05	hierarchical porous	50	877.9	[173]
Porous graphene film	10	porous structure	10,000	971	[140]
3D multilayer-graphene	5	cloud-like	1100	260.3	[111]
N-doped carbon nanospheres	0.1	nanospheres	150	505	[174]
N-doped graphene	0.1	nanosheets	100	452	[175]
Hierarchical porous Carbon microspheres	1	hierarchical porous microspheres	70	200	[127]
C-Co ₉ S ₈	2	hierarchical porous	400	476	[161]
MnCo ₂ O ₄ /C	0.05	quasi-hollow microspheres	50	488	[56]
Co ₃ O ₄ /APC (Activated porous carbon)	0.5	lotus root-like and layered porous	200	625	[20]
Co/CPC (CO ₂ -derived porous carbon)	1	porous	300	1179	[19]
Co ₃ O ₄ @CNT	0.01	mesoporous peapod-like	100	700	[176]
Co ₃ O ₄ @Graphene core-shell	1	mesoporous hollow spheres	200	700	[18]
CoO-Co ₃ O ₄ -RGO	0.1	sandwich-like	200	994	[177]
Carbon@cobaltous oxide	0.2	nanofiber	100	892	[17]
CoP@C	0.5	uniform spherical morphology	1000	483.4	[178]
Co _{1-x} S-CNFs	2	onion-like carbonaceous	500	252	[179]

5. Summary and Outlook

Generally speaking, this paper summarizes the progress and challenges of the application of cobalt nanomaterials, carbon nanomaterials, and their composites in lithium-ion batteries. In the research of lithium batteries, the Co₃O₄ anode has excellent performance, which can significantly improve the performance of LIBs. However, the shortcomings of fast capacity attenuation and low rates of performance limit its practical application. The difference is that binary cobalt-containing oxides and cobalt-containing sulfides have higher specific capacitance than Co₃O₄, and their volume changes during charge and discharge can be reduced by adjusting their micro-morphology or compounding with other materials, thus improving their electrochemical cycle performance. As the traditional anode materials in electrochemical energy storage devices, carbon nanotubes, carbon nanosheets, carbon nanospheres, graphene, and other carbonaceous materials still occupy an irreplaceable position in the application of lithium-ion batteries. At present, the composite of cobalt-containing nanomaterials and carbon materials is one of the main means to improve the electrochemical performance of cobalt nanomaterials. The synergistic effect between them can effectively improve the properties of composites, which have excellent electrochemical performance as anodes of lithium-ion batteries.

Nano-sized cobalt-containing compounds have rich natural reserves, strong electrical conductivity, and large theoretical specific capacitance. In the past twenty years, they have been widely used and developed. Although there are some shortcomings in practical application, such as low energy density and short cycle life, their electrochemical performance has been significantly improved by various methods. Moreover, with the

continuous improvement of researchers' proficiency with regard to the production process, nano-cobalt-containing compounds have been used in commercial fields. Carbon nanomaterials also show excellent performance as anode materials for lithium-ion batteries. In the future, it will be necessary to further explore methods to accurately control their morphology and structure. At the same time, while ensuring their electrochemical performance, the preparation process should be simplified, and the cost should be reduced as much as possible.

It should also be noted that although cobalt resources are abundant at present, some scholars have predicted that they may not be able to meet demand by around 2050. Therefore, in order to ensure the further research and the sustainable utilization of cobalt-containing nanomaterials, it is of great significance to add other metals appropriately to reduce the usage of cobalt while ensuring the performance of batteries, and to further develop the recycling and utilization technology of lithium-ion batteries.

Author Contributions: Writing—original draft preparation and data curation, H.C., W.W., M.L. and L.Y.; writing—review and editing, H.W., L.D., D.W. (Dechen Wang), X.X., D.W. (Dijia Wang) and J.H.; supervision, H.W.; project administration, H.W.; funding acquisition, H.W. All authors have read and agreed to the published version of the manuscript.

Funding: This work was supported by the Natural Science Foundation of China under Grant 21604007.

Institutional Review Board Statement: Not applicable.

Informed Consent Statement: Not applicable.

Data Availability Statement: Not applicable.

Conflicts of Interest: The authors declare no conflict of interest.

References

1. Liu, R.; Zhou, A. Fundamentals, Advances and Challenges of Transition Metal Compounds-based Supercapacitors. *Chem. Eng. J.* **2021**, *412*, 128611. [[CrossRef](#)]
2. Wang, X.; Zhang, J.; Yang, S.; Yan, H.; Hong, X.; Dong, W.; Liu, Y.; Zhang, B.; Wen, Z. Interlayer space regulating of NiMn layered double hydroxides for supercapacitors by controlling hydrothermal reaction time. *Electrochim. Acta* **2019**, *295*, 1–6. [[CrossRef](#)]
3. Palacin, M.R. Recent advances in rechargeable battery materials: A chemist's perspective. *Chem. Soc. Rev.* **2009**, *38*, 2565–2575. [[CrossRef](#)] [[PubMed](#)]
4. Ji, L.; Lin, Z.; Alcoutlabi, M.; Zhang, X. Recent developments in nanostructured anode materials for rechargeable lithium-ion batteries. *Energy Environ. Sci.* **2011**, *4*, 2682–2699. [[CrossRef](#)]
5. Li, W.; Zhang, B. A Dendritic Nickel Cobalt Sulfide Nanostructure for Alkaline Battery Electrodes. *Adv. Funct. Mater.* **2018**, *28*, 1705937. [[CrossRef](#)]
6. Koksang, R.; Barker, J. Cathode materials for lithium rocking chair batteries. *Solid State Ion.* **1996**, *3*, 1–21. [[CrossRef](#)]
7. Islam, M.S.; Fisher, C.A. Lithium and sodium battery cathode materials: Computational insights into voltage, diffusion and nanostructural properties. *Chem. Soc. Rev.* **2014**, *43*, 185–204. [[CrossRef](#)]
8. Ding, Y.; Cano, Z.P. Automotive Li-Ion Batteries: Current Status and Future Perspectives. *Electrochem. Energy Rev.* **2019**, *2*, 1–28. [[CrossRef](#)]
9. Andre, D.; Kim, S.J. Future generations of cathode materials: An automotive industry perspective. *J. Mater. Chem. A* **2015**, *3*, 6709–6732. [[CrossRef](#)]
10. Liu, Q.; Su, X. Approaching the capacity limit of lithium cobalt oxide in lithium ion batteries via lanthanum and aluminium doping. *Nat. Energy* **2018**, *3*, 936–943. [[CrossRef](#)]
11. Kang, Y.; Zhang, Y.H. Highly efficient $\text{Co}_3\text{O}_4/\text{CeO}_2$ heterostructure as anode for lithium-ion batteries. *J. Colloid. Interface Sci.* **2021**, *585*, 705–715. [[CrossRef](#)] [[PubMed](#)]
12. Islam, M.; Akbar, M. A high voltage Li-ion full-cell battery with $\text{MnCo}_2\text{O}_4/\text{LiCoPO}_4$ electrodes. *Ceram. Int.* **2020**, *46*, 26147–26155. [[CrossRef](#)]
13. Liang, L.; Li, J. Cobalt Chalcogenides/Cobalt Phosphides/Cobaltates with Hierarchical Nanostructures for Anode Materials of Lithium-Ion Batteries: Improving the Lithiation Environment. *Small* **2021**, *17*, e1903418. [[CrossRef](#)] [[PubMed](#)]
14. Aboelazm, E.A.A.; Ali, G.A.M.; Algarni, H.; Yin, H.; Zhong, Y.L.; Chong, K.F. Magnetic Electrodeposition of the Hierarchical Cobalt Oxide Nanostructure from Spent Lithium-Ion Batteries: Its Application as a Supercapacitor Electrode. *J. Phys. Chem. C* **2018**, *122*, 12200–12206. [[CrossRef](#)]
15. Ali, G.A.; Fouad, O.A. $\text{Co}_3\text{O}_4/\text{SiO}_2$ nanocomposites for supercapacitor application. *Electrochemistry* **2014**, *18*, 2505–2512. [[CrossRef](#)]

16. Ali, G.; Habeeb, O.A. CaO impregnated highly porous honeycomb activated carbon from agriculture waste symmetrical supercapacitor study. *J. Mater. Sci.* **2019**, *54*, 683–692. [[CrossRef](#)]
17. Lei, T.; Wang, Y.; Pan, F.; Dang, B. Nanofibrous carbon@cobaltous oxide composites for high electrochemical performance as anode materials of lithium-ion batteries. *Ionics* **2021**, *27*, 5097–5101. [[CrossRef](#)]
18. Sun, H.; Sun, X.; Hu, T.; Yu, M.; Lu, F.; Lian, J. Graphene-Wrapped Mesoporous Cobalt Oxide Hollow Spheres Anode for High-Rate and Long-Life Lithium Ion Batteries. *J. Phys. Chem. C* **2014**, *118*, 2263–2272. [[CrossRef](#)]
19. Choi, W.Y.; Lee, D.K. Cobalt oxide-porous carbon composite derived from CO₂ for the enhanced performance of lithium-ion battery. *J. CO₂ Util.* **2019**, *30*, 28–37. [[CrossRef](#)]
20. Gu, F.; Liu, W. Small Co₃O₄/waste pinecone-derived activated porous carbon as anode materials of lithium-ion batteries. *Ionics* **2020**, *26*, 5897–5906. [[CrossRef](#)]
21. Gangulibabu; Nallathamby, K. Carbonate anion controlled growth of LiCoPO₄/C nanorods and its improved electrochemical behavior. *Electrochim. Acta* **2013**, *101*, 18–26. [[CrossRef](#)]
22. Kim, D.H.; Park, G.D. Electrochemical properties of yolk-shell structured cobalt hydroxy chloride-carbon composite as an anode for lithium-ion batteries. *Int. J. Energy Reseach* **2022**, *46*, 9761–9770. [[CrossRef](#)]
23. Xu, K.; Shen, X. Cyanometallic framework-derived dual-buffer structure of Sn-Co based nanocomposites for high-performance lithium storage. *J. Alloy. Compd.* **2020**, *830*, 154680. [[CrossRef](#)]
24. Umirov, N.; Seo, D.-H. Microstructure and electrochemical properties of rapidly solidified Si–Ni alloys as anode for lithium-ion batteries. *J. Ind. Eng. Chem.* **2019**, *71*, 351–360. [[CrossRef](#)]
25. Wan, H.; Hu, X. Sulfur-doped honeycomb-like carbon with outstanding electrochemical performance as an anode material for lithium and sodium ion batteries. *J. Colloid Interface Sci.* **2020**, *558*, 242–250. [[CrossRef](#)]
26. Zhang, H.; Hu, M. Monodisperse nitrogen-doped carbon spheres with superior rate capacities for lithium/sodium ion storage. *Electrochim. Acta* **2019**, *297*, 365–371. [[CrossRef](#)]
27. Zheng, Z.; Li, P. High performance columnar-like Fe₂O₃@carbon composite anode via yolk@shell structural design. *J. Energy Chem.* **2020**, *41*, 126–134. [[CrossRef](#)]
28. Shi, M.; Huang, Z. Ultralow nitrogen-doped carbon coupled carbon-doped Co₃O₄ microrods with tunable electron configurations for advanced Li-storage properties. *Electrochim. Acta* **2019**, *327*, 135059. [[CrossRef](#)]
29. Elizabeth, I.; Singh, B.P. Electrochemical performance of Sb₂S₃/CNT free-standing flexible anode for Li-ion batteries. *J. Mater. Sci.* **2019**, *54*, 7110–7118. [[CrossRef](#)]
30. Zhang, Q.; Liao, J. One-dimensional Fe₇S₈@C nanorods as anode materials for high-rate and long-life lithium-ion batteries. *Appl. Surf. Sci.* **2019**, *473*, 799–806. [[CrossRef](#)]
31. Song, X.Y.; Zhang, Y.H. Lithium-Lanthanide Bimetallic Metal-Organic Frameworks towards Negative Electrode Materials for Lithium-Ion Batteries. *Chemistry* **2020**, *26*, 5654–5661. [[CrossRef](#)] [[PubMed](#)]
32. Pan, G.-X.; Zhang, Y.-H. A brand-new bimetallic copper-lithium HEDP complex of fast ion migration as a promising anode for lithium ion batteries. *J. Mol. Struct.* **2020**, *1214*, 128223. [[CrossRef](#)]
33. Biswal, A.; Panda, P. Facile synthesis of a nanoporous sea sponge architecture in a binary metal oxide. *Nanoscale Adv.* **2019**, *1*, 1880–1892. [[CrossRef](#)]
34. Albohani, S.; Sundaram, M.M.; Laird, D.W. Egg shell membrane template stabilises formation of β-NiMoO₄ nanowires and enhances hybrid supercapacitor behaviour. *Mater. Lett.* **2018**, *236*, 64–68. [[CrossRef](#)]
35. Minakshi, M.; Mitchell, D. Phase evolution in calcium molybdate nanoparticles as a function of synthesis temperature and its electrochemical effect on energy storage. *Nanoscale Adv.* **2018**, *1*, 565–580. [[CrossRef](#)]
36. Reddy, M.V.; Subba Rao, G.V. Metal oxides and oxysalts as anode materials for Li ion batteries. *Chem. Rev.* **2013**, *113*, 5364–5457. [[CrossRef](#)]
37. Poizot, P.; Dupont, L.; Laruelle, S. Nano-sized transition-metal oxides as negative-electrode materials for lithium-ion batteries. *Nature* **2000**, *9*, 496–499. [[CrossRef](#)]
38. Baji, D.S.; Nair, S.V. Highly porous disk-like shape of Co₃O₄ as an anode material for lithium ion batteries. *J. Solid State Electrochem.* **2017**, *21*, 2869–2875. [[CrossRef](#)]
39. Li, L.; Jiang, G. Two-dimensional porous Co₃O₄ nanosheets for high-performance lithium ion batteries. *New J. Chem.* **2017**, *41*, 15283–15288. [[CrossRef](#)]
40. Zhang, C.; Ke, F. Well-designed hollow and porous Co₃O₄ microspheres used as an anode for Li-ion battery. *J. Solid State Electrochem.* **2019**, *23*, 2477–2482. [[CrossRef](#)]
41. Li, J.; Li, Z. Ultrathin Mesoporous Co₃O₄ Nanosheet Arrays for High-Performance Lithium-Ion Batteries. *ACS Omega* **2018**, *3*, 1675–1683. [[CrossRef](#)] [[PubMed](#)]
42. Divakaran, A.M.; Minakshi, M.; Bahri, P.A.; Paul, S.; Kumari, P.; Divakaran, A.M.; Manjunatha, K.N. Rational design on materials for developing next generation lithium-ion secondary battery. *Prog. Solid State Chem.* **2020**, *62*, 100298. [[CrossRef](#)]
43. Bai, J.; Li, X. Unusual Formation of ZnCo₂O₄ 3D Hierarchical Twin Microspheres as a High-Rate and Ultralong-Life Lithium-Ion Battery Anode Material. *Adv. Funct. Mater.* **2014**, *24*, 3012–3020. [[CrossRef](#)]
44. Sharma, Y.; Sharma, N. Studies on spinel cobaltites, FeCo₂O₄ and MgCo₂O₄ as anodes for Li-ion batteries. *Solid State Ion.* **2008**, *179*, 587–597. [[CrossRef](#)]
45. Li, T.; Li, X. A novel NiCo₂O₄ anode morphology for lithium-ion batteries. *J. Mater. Chem. A* **2015**, *3*, 11970–11975. [[CrossRef](#)]

46. Badway, F.; Plitz, I. Metal Oxides as Negative Electrode Materials in Li-Ion Cells. *Electrochem. Solid-State Lett.* **2002**, *5*, A115. [[CrossRef](#)]
47. Jin, R.; Ma, Y. Manganese Cobalt Oxide (MnCo₂O₄) Hollow Spheres as High Capacity Anode Materials for Lithium-Ion Batteries. *Energy Technol.* **2017**, *5*, 293–299. [[CrossRef](#)]
48. Jin, Y.; Wang, L. Mesoporous MnCo₂O₄ microflower constructed by sheets for lithium ion batteries. *Mater. Lett.* **2016**, *177*, 85–88. [[CrossRef](#)]
49. Kong, X.; Zhu, T. Uniform MnCo₂O₄ Porous Dumbbells for Lithium-Ion Batteries and Oxygen Evolution Reactions. *ACS Appl. Mater. Interfaces* **2018**, *10*, 8730–8738. [[CrossRef](#)]
50. Chen, C.; Liu, B.; Ru, Q.; Ma, S.; An, B.; Hou, X.; Hu, S. Fabrication of cubic spinel MnCo₂O₄ nanoparticles embedded in graphene sheets with their improved lithium-ion and sodium-ion storage properties. *J. Power Sources* **2016**, *326*, 252–263. [[CrossRef](#)]
51. Ding, R.; Li, Z.; Wang, C.; Chen, M. Porous MnCo₂O₄-TiO₂ microspheres with a yolk-shell structure for lithium-ion battery applications. *J. Alloy. Compd.* **2017**, *726*, 445–452. [[CrossRef](#)]
52. Fu, C.; Li, G. One-step calcination-free synthesis of multicomponent spinel assembled microspheres for high-performance anodes of li-ion batteries: A case study of MnCo₂O₄. *ACS Appl. Mater. Interfaces* **2014**, *6*, 2439–2449. [[CrossRef](#)] [[PubMed](#)]
53. Huang, G.; Xu, S.; Xu, Z.; Sun, H.; Li, L. Core-shell ellipsoidal MnCo₂O₄ anode with micro-/nano-structure and concentration gradient for lithium-ion batteries. *ACS Appl. Mater. Interfaces* **2014**, *6*, 21325–21334. [[CrossRef](#)] [[PubMed](#)]
54. Zhang, Y.; Wang, X. Facile preparation and performance of hierarchical self-assembly MnCo₂O₄ nanoflakes as anode active material for lithium ion batteries. *Electrochim. Acta* **2015**, *180*, 866–872. [[CrossRef](#)]
55. Zhou, S.; Luo, X. MnCo₂O₄ nanospheres for improved lithium storage performance. *Ceram. Int.* **2018**, *44*, 17858–17863. [[CrossRef](#)]
56. Yun, Y.J.; Kim, J.K. A morphology, porosity and surface conductive layer optimized MnCo₂O₄ microsphere for compatible superior Li⁺ ion/air rechargeable battery electrode materials. *Dalton Trans.* **2016**, *45*, 5064–5070. [[CrossRef](#)]
57. Li, G.; Xu, L.; Zhai, Y.; Hou, Y. Fabrication of hierarchical porous MnCo₂O₄ and CoMn₂O₄ microspheres composed of polyhedral nanoparticles as promising anodes for long-life LIBs. *J. Mater. Chem. A* **2015**, *3*, 14298–14306. [[CrossRef](#)]
58. Xu, H.; Shen, H.; Song, X.; Kong, X.; Zhang, Y.; Qin, Z. Hydrothermal synthesis of porous hydrangea-like MnCo₂O₄ as anode materials for high performance lithium ion batteries. *J. Electroanal. Chem.* **2019**, *851*, 113455. [[CrossRef](#)]
59. Zeng, P.; Wang, X. Excellent lithium ion storage property of porous MnCo₂O₄ nanorods. *RSC Adv.* **2016**, *6*, 23074–23084. [[CrossRef](#)]
60. Zhang, L.; Tang, Q. Self-assembled synthesis of diamond-like MnCo₂O₄ as anode active material for lithium-ion batteries with high cycling stability. *J. Alloy. Compd.* **2017**, *722*, 387–393. [[CrossRef](#)]
61. Wu, W.; Wang, K. Synthesis and electrochemical performance of flower-like MnCo₂O₄ as an anode material for sodium ion batteries. *Mater. Lett.* **2015**, *147*, 85–87. [[CrossRef](#)]
62. Li, J.; Wang, J.; Liang, X.; Zhang, Z.; Liu, H.; Qian, Y.; Xiong, S. Hollow MnCo₂O₄ Submicrospheres with Multilevel Interiors: From Mesoporous Spheres to Yolk-in-Double-Shell Structures. *ACS Appl. Mater. Interfaces* **2013**, *6*, 24–30. [[CrossRef](#)] [[PubMed](#)]
63. Xu, X.; Cao, K. 3D hierarchical porous ZnO/ZnCo₂O₄ nanosheets as high-rate anode material for lithium-ion batteries. *J. Mater. Chem. A* **2016**, *4*, 6042–6047. [[CrossRef](#)]
64. Wu, M.; Leung, D.Y.C. Toluene degradation over Mn-TiO₂/CeO₂ composite catalyst under vacuum ultraviolet (VUV) irradiation. *Chem. Eng. Sci.* **2019**, *195*, 985–994. [[CrossRef](#)]
65. Yang, X.; Wang, Y. Interior Supported Hierarchical TiO₂@Co₃O₄ Derived from MOF-on-MOF Architecture with Enhanced Electrochemical Properties for Lithium Storage. *ChemElectroChem* **2019**, *6*, 3657–3666. [[CrossRef](#)]
66. Zhao, J.; Yao, S. Porous ZnO/Co₃O₄/CoO/Co composite derived from Zn-Co-ZIF as improved performance anodes for lithium-ion batteries. *Mater. Lett.* **2019**, *250*, 75–78. [[CrossRef](#)]
67. Liu, H.; Wu, X. Tailored Synthesis of Coral-Like CoTiO₃/Co₃O₄/TiO₂ Nanobelts with Superior Lithium Storage Capability. *Energy Technol.* **2019**, *8*, 1900774. [[CrossRef](#)]
68. Liu, H.; Cao, K. Constructing hierarchical MnO₂/Co₃O₄ heterostructure hollow spheres for high-performance Li-Ion batteries. *J. Power Sources* **2019**, *437*, 226904. [[CrossRef](#)]
69. Zhong, M.; Yang, D.H. Bimetallic metal-organic framework derived Co₃O₄-CoFe₂O₄ composites with different Fe/Co molar ratios as anode materials for lithium ion batteries. *Dalton Trans.* **2017**, *46*, 15947–15953. [[CrossRef](#)]
70. Ding, H.; Zhang, X.K. MOF-Templated Synthesis of Co₃O₄@TiO₂ Hollow Dodecahedrons for High-Storage-Density Lithium-Ion Batteries. *ACS Omega* **2019**, *4*, 13241–13249. [[CrossRef](#)]
71. Wang, P.; Zhang, P. Constructing MoS₂/CoMo₂S₄/Co₃S₄ nanostructures supported by graphene layers as the anode for lithium-ion batteries. *Dalton Trans.* **2020**, *49*, 1167–1172. [[CrossRef](#)] [[PubMed](#)]
72. Chen, G.; Ma, W. Shape evolution and electrochemical properties of cobalt sulfide via a biomolecule-assisted solvothermal route. *Solid State Sci.* **2013**, *17*, 102–106. [[CrossRef](#)]
73. Zhou, Y.; Yan, D. Hollow nanospheres of mesoporous Co₉S₈ as a high-capacity and long-life anode for advanced lithium ion batteries. *Nano Energy* **2015**, *12*, 528–537. [[CrossRef](#)]
74. Zhang, X.; Sun, Y. Nanosized SnO₂-CoS constructed porous cubeas advanced lithium-ion batteries anode. *Ceram. Int.* **2018**, *44*, 5569–5571. [[CrossRef](#)]
75. Yang, S.H.; Park, S.-K. A MOF-mediated strategy for constructing human backbone-like CoMoS₃@N-doped carbon nanostructures with multiple voids as a superior anode for sodium-ion batteries. *J. Mater. Chem. A* **2019**, *7*, 13751–13761. [[CrossRef](#)]

76. Yu, D.J.; Yuan, Y.F. Nickel cobalt sulfide Nanotube Array on Nickel Foam as Anode Material for Advanced Lithium-Ion Batteries. *Electrochim. Acta* **2016**, *198*, 280–286. [[CrossRef](#)]
77. Wang, Y.; Zhang, Y. Physical confinement and chemical adsorption of porous C/CNT micro/nano-spheres for CoS and Co₉S₈ as advanced lithium batteries anodes. *Electrochim. Acta* **2019**, *299*, 489–499. [[CrossRef](#)]
78. Wang, H.; Ma, J. CoS/CNTs hybrid structure for improved performance lithium ion battery. *J. Alloy. Compd.* **2016**, *676*, 551–556. [[CrossRef](#)]
79. Li, X.; Fu, N. Ultrafine Cobalt Sulfide Nanoparticles Encapsulated Hierarchical N-doped Carbon Nanotubes for High-performance Lithium Storage. *Electrochim. Acta* **2017**, *225*, 137–142. [[CrossRef](#)]
80. Yao, Y.; Zhu, Y. Porous CoS nanosheets coated by N and S doped carbon shell on graphene foams for free-standing and flexible lithium ion battery anodes: Influence of void spaces, shell and porous nanosheet. *Electrochim. Acta* **2018**, *271*, 242–251. [[CrossRef](#)]
81. Gu, Y.; Xu, Y. Graphene-wrapped CoS nanoparticles for high-capacity lithium-ion storage. *ACS Appl. Mater. Interfaces* **2013**, *5*, 801–806. [[CrossRef](#)] [[PubMed](#)]
82. Zhu, J.; Ding, X. Embedding cobalt sulfide in reduced graphene oxide for superior lithium-ion storage. *Mater. Lett.* **2019**, *253*, 22–25. [[CrossRef](#)]
83. Ni, J.; Li, Y. Carbon Nanomaterials in Different Dimensions for Electrochemical Energy Storage. *Adv. Energy Mater.* **2016**, *6*, 1600278. [[CrossRef](#)]
84. Goriparti, S.; Miele, E. Review on recent progress of nanostructured anode materials for Li-ion batteries. *J. Power Sources* **2014**, *257*, 421–443. [[CrossRef](#)]
85. Gu, J.; Du, Z. Pyridinic Nitrogen-Enriched Carbon Nanogears with Thin Teeth for Superior Lithium Storage. *Adv. Energy Mater.* **2016**, *6*, 1600917. [[CrossRef](#)]
86. Lee, S.W.; Yabuuchi, N. High-power lithium batteries from functionalized carbon-nanotube electrodes. *Nat. Nanotechnol.* **2010**, *5*, 531–537. [[CrossRef](#)]
87. Fan, Z.; Yan, J. A Three-Dimensional Carbon Nanotube/Graphene Sandwich and Its Application as Electrode in Supercapacitors. *Adv. Mater.* **2010**, *22*, 3723. [[CrossRef](#)]
88. Qie, L.; Chen, W.-M. Nitrogen-Doped Porous Carbon Nanofiber Webs as Anodes for Lithium Ion Batteries with a Superhigh Capacity and Rate Capability. *Adv. Mater.* **2012**, *24*, 2047–2050. [[CrossRef](#)]
89. Zheng, G.; Yang, Y. Hollow Carbon Nanofiber-Encapsulated Sulfur Cathodes for High Specific Capacity Rechargeable Lithium Batteries. *Nano Lett.* **2011**, *11*, 4462–4467. [[CrossRef](#)]
90. Lian, P.; Zhu, X. Large reversible capacity of high quality graphene sheets as an anode material for lithium-ion batteries. *Electrochim. Acta* **2010**, *55*, 3909–3914. [[CrossRef](#)]
91. Liu, F.; Song, S. Folded Structured Graphene Paper for High Performance Electrode Materials. *Adv. Mater.* **2012**, *24*, 1089–1094. [[CrossRef](#)] [[PubMed](#)]
92. Lee, R.S.; Kim, H.J. Conductivity enhancement in single-walled carbon nanotube bundles doped with K and Br. *Nature* **1997**, *388*, 255–257. [[CrossRef](#)]
93. Yang, S.; Song, H. Electrochemical performance of arc-produced carbon nanotubes as anode material for lithium-ion batteries. *Electrochim. Acta* **2007**, *52*, 5286–5293. [[CrossRef](#)]
94. Eom, J.; Kim, D. Effects of ball-milling on lithium insertion into multi-walled carbon nanotubes synthesized by thermal chemical vapour deposition. *J. Power Sources* **2006**, *157*, 507–514. [[CrossRef](#)]
95. Gao, B.; Bower, C. Enhanced saturation lithium composition in ball-milled single-walled carbon nanotubes. *Chem. Phys. Lett.* **2000**, *327*, 69–75. [[CrossRef](#)]
96. Yang, S.; Huo, J. A comparative study of electrochemical properties of two kinds of carbon nanotubes as anode materials for lithium ion batteries. *Electrochim. Acta* **2008**, *53*, 2238–2244. [[CrossRef](#)]
97. Bulusheva, L.; Arkhipov, V.; Fedorovskaya, E.; Zhang, S.; Kurenin, A.; Kanygin, M.; Asanov, I.; Tsygankova, A.; Chen, X.; Song, H.; et al. Fabrication of free-standing aligned multiwalled carbon nanotube array for Li-ion batteries. *J. Power Sources* **2016**, *311*, 42–48. [[CrossRef](#)]
98. Novoselov, K.S.; Geim, A.K. Two-Dimensional Gas of Massless Dirac Fermions in Graphene. *Nature* **2005**, *438*, 197–200. [[CrossRef](#)]
99. Kyun, K.D.; Kim, T. A Review: Comparison of Fabrication and Characteristics of Flexible ReRAM and Multi-Insulating Graphene Oxide Layer ReRAM. *Trans. Korean Inst. Electr. Eng.* **2016**, *65*, 1369–1375.
100. Song, N.; Gao, X. A review of graphene-based separation membrane: Materials, characteristics, preparation and applications. *Desalination* **2018**, *437*, 59–72. [[CrossRef](#)]
101. Gangu, K.K.; Maddila, S. Characteristics of MOF, MWCNT and graphene containing materials for hydrogen storage: A review. *J. Energy Chem.* **2019**, *30*, 132–144. [[CrossRef](#)]
102. Chen, J.; Lin, Y. Three-dimensional hierarchical nanocomposites of NiSnO₃/graphene encapsulated in carbon matrix as long-life anode for lithium-ion batteries. *J. Alloy. Compd.* **2019**, *793*, 492–498. [[CrossRef](#)]
103. Ju, J.Y.; Ji, S. Rational design of electrochemically active polymorphic MnO_x/rGO composites for Li⁺-rechargeable battery electrodes. *Ceram. Int.* **2019**, *45*, 9522–9528. [[CrossRef](#)]
104. Shenouda, A.Y.; Momchilov, A.A. A study on graphene/tin oxide performance as negative electrode compound for lithium battery application. *J. Mater. Sci. Mater. Electron.* **2019**, *30*, 79–90. [[CrossRef](#)]

105. Wu, Q.; Jiang, R. Carbon layer encapsulated Fe₃O₄@Reduced graphene oxide lithium battery anodes with long cycle performance. *Ceram. Int.* **2020**, *46*, 12732–12739. [[CrossRef](#)]
106. Lochala, J.A.; Zhang, H. Practical Challenges in Employing Graphene for Lithium-Ion Batteries and Beyond. *Small Methods* **2017**, *1*, 1700099. [[CrossRef](#)]
107. Mei, R.; Song, X. Hollow reduced graphene oxide microspheres as a high-performance anode material for Li-ion batteries. *Electrochim. Acta* **2015**, *153*, 540–545. [[CrossRef](#)]
108. Wei, T.; Wang, F. Microspheres composed of multilayer graphene as anode material for lithium-ion batteries. *J. Electroanal. Chem.* **2011**, *653*, 45–49. [[CrossRef](#)]
109. Guo, P.; Song, H. Electrochemical performance of graphene nanosheets as anode material for lithium-ion batteries. *Electrochem. Commun.* **2009**, *11*, 1320–1324. [[CrossRef](#)]
110. Song, R.; Cao, B. A simple preparation of porous graphene nanosheets containing onion-like nano-holes with favorable high-rate Li-storage performance. *RSC Adv.* **2016**, *6*, 63373–63377. [[CrossRef](#)]
111. Rish, S.K.; Tahmasebi, A. Novel composite nano-materials with 3D multilayer-graphene structures from biomass-based activated-carbon for ultrahigh Li-ion battery performance. *Electrochim. Acta* **2021**, *390*, 138839. [[CrossRef](#)]
112. Luo, W.-B.; Chou, S.-L. Self-assembled graphene and LiFePO₄ composites with superior high rate capability for lithium ion batteries. *J. Mater. Chem. A* **2014**, *2*, 4927–4931. [[CrossRef](#)]
113. Zhou, X.; Wang, F. Graphene modified LiFePO₄ cathode materials for high power lithium ion batteries. *J. Mater. Chem.* **2011**, *21*, 3353–3358. [[CrossRef](#)]
114. Xu, Z.; Gao, L. Review-Recent Developments in the Doped LiFePO₄ Cathode Materials for Power Lithium Ion Batteries. *J. Electrochem. Soc.* **2016**, *163*, A2600–A2610. [[CrossRef](#)]
115. Li, L.; Wu, L. Review-Recent Research Progress in Surface Modification of LiFePO₄ Cathode Materials. *J. Electrochem. Soc.* **2017**, *164*, A2138–A2150. [[CrossRef](#)]
116. Zhu, H.; Wu, X. Three-Dimensional Macroporous Graphene-Li₂FeSiO₄ Composite as Cathode Material for Lithium-Ion Batteries with Superior Electrochemical Performances. *ACS Appl. Mater. Interfaces* **2014**, *6*, 11724–11733. [[CrossRef](#)]
117. Liu, J.; Wickramaratne, N.P. Molecular-based design and emerging applications of nanoporous carbon spheres. *Nat. Mater.* **2015**, *14*, 763–774. [[CrossRef](#)]
118. Park, S.-H.; Kim, H.-K. Spray-Assisted Deep-Frying Process for the In Situ Spherical Assembly of Graphene for Energy-Storage Devices. *Chem. Mater.* **2015**, *27*, 457–465. [[CrossRef](#)]
119. Shi, J.-L.; Peng, H.-J.; Zhu, L.; Zhu, W.; Zhang, Q. Template growth of porous graphene microspheres on layered double oxide catalysts and their applications in lithium–sulfur batteries. *Carbon* **2000**, *92*, 96–105. [[CrossRef](#)]
120. Li, D.; Chen, H. Porous nitrogen doped carbon sphere as high performance anode of sodium-ion battery. *Carbon* **2015**, *94*, 888–894. [[CrossRef](#)]
121. Xu, S.; Zhang, Z.; Wu, T.; Xue, Y. Nanoporous carbon microspheres as anode material for enhanced capacity of lithium ion batteries. *Ionics* **2018**, *24*, 99–109. [[CrossRef](#)]
122. Yi, R.; Dai, F. Micro-sized Si-C Composite with Interconnected Nanoscale Building Blocks as High-Performance Anodes for Practical Application in Lithium-Ion Batteries. *Adv. Energy Mater.* **2013**, *3*, 295–300. [[CrossRef](#)]
123. Chen, T.; Pan, L. Porous nitrogen-doped carbon microspheres as anode materials for lithium ion batteries. *Dalton Trans.* **2014**, *43*, 14931–14935. [[CrossRef](#)] [[PubMed](#)]
124. Wang, Q.; Li, H. Novel spherical microporous carbon as anode material for Li-ion batteries. *Solid State Ion.* **2002**, *152*, 43–50. [[CrossRef](#)]
125. Hu, Y.-S.; Adelhelm, P. Synthesis of hierarchically porous carbon monoliths with highly ordered microstructure and their application in rechargeable lithium batteries with high-rate capability. *Adv. Funct. Mater.* **2007**, *17*, 1873–1878. [[CrossRef](#)]
126. Zhang, F.; Wang, K.-X. Hierarchical porous carbon derived from rice straw for lithium ion batteries with high-rate performance. *Electrochem. Commun.* **2009**, *11*, 130–133. [[CrossRef](#)]
127. Wang, F.; Song, R.; Song, H.; Chen, X.; Zhou, J.; Ma, Z.; Li, M.; Lei, Q. Simple synthesis of novel hierarchical porous carbon microspheres and their application to rechargeable lithium-ion batteries. *Carbon* **2015**, *81*, 314–321. [[CrossRef](#)]
128. Etacheri, V.; Wang, C.; O’Connell, M.J.; Chan, C.K.; Pol, V. GPorous carbon sphere anodes for enhanced lithium-ion storage. *J. Mater. Chem. A* **2015**, *3*, 9861–9868. [[CrossRef](#)]
129. Shi, L.; Chen, Y. Fabrication of hierarchical porous carbon microspheres using porous layered double oxide templates for high-performance lithium ion batteries. *Carbon* **2017**, *123*, 186–192. [[CrossRef](#)]
130. Zhang, L.; Dou, Y.; Guo, H.; Zhang, B.; Liu, X.; Wan, M.; Li, W.; Hu, X.; Dou, S.; Huang, Y.; et al. A facile way to fabricate double-shell pomegranate-like porous carbon microspheres for high-performance Li-ion batteries. *J. Mater. Chem. A* **2017**, *5*, 12073–12079. [[CrossRef](#)]
131. Zhang, C.; Wu, Z.; Jan, S.; Wang, Z.; Bennaceur, S.; Kim, H.-K.; Jin, X. Glucose-derived hollow microsphere graphite with a nanosheets-constructed porous shell for improved lithium storage. *Electrochim. Acta* **2021**, *390*, 138800. [[CrossRef](#)]
132. Bagri, P.; Thapaliya, B.P. Electrochemically induced crystallization of amorphous materials in molten MgCl₂: Boron nitride and hard carbon. *Chem. Commun.* **2020**, *56*, 2783–2786. [[CrossRef](#)] [[PubMed](#)]
133. Tu, J.; Wang, J. High-efficiency transformation of amorphous carbon into graphite nanoflakes for stable aluminum-ion battery cathodes. *Nanoscale* **2019**, *11*, 12537–12546. [[CrossRef](#)] [[PubMed](#)]

134. Zhu, Z.; Zuo, H. A green electrochemical transformation of inferior coals to crystalline graphite for stable Li-ion storage. *J. Mater. Chem. A* **2019**, *7*, 7533–7540. [[CrossRef](#)]
135. Song, W.-L.; Li, S. Cellulose-derived flake graphite as positive electrodes for Al-ion batteries. *Sustain. Energy Fuels* **2019**, *3*, 3561–3568. [[CrossRef](#)]
136. Zhang, C.; He, R. Amorphous Carbon-Derived Nanosheet-Bricked Porous Graphite as High-Performance Cathode for Aluminum-Ion Batteries. *ACS Appl. Mater. Interfaces* **2018**, *10*, 26510–26516. [[CrossRef](#)]
137. Jin, X.; He, R.; Dai, S. Frontispiece: Electrochemical Graphitization: An Efficient Conversion of Amorphous Carbons to Nanostructured Graphites. *Chem. A Eur. J.* **2017**, *23*, 11455–11459. [[CrossRef](#)]
138. Peng, J.; Chen, N. Electrochemically Driven Transformation of Amorphous Carbons to Crystalline Graphite Nanoflakes: A Facile and Mild Graphitization Method. *Angew. Chem. Int. Ed.* **2017**, *56*, 1751–1755. [[CrossRef](#)]
139. Xie, Q.; Qu, S. Nitrogen-enriched graphene-like carbon architecture with tunable porosity derived from coffee ground as high performance anodes for lithium ion batteries. *Appl. Surf. Sci.* **2021**, *537*, 148092. [[CrossRef](#)]
140. Zhang, X.; Zhou, J.; Liu, C.; Chen, X.; Song, H. A universal strategy to prepare porous graphene films: Binder-free anodes for high-rate lithium-ion and sodium-ion batteries. *J. Mater. Chem. A* **2016**, *4*, 8837–8843. [[CrossRef](#)]
141. Ahn, W.; Song, H.S.; Park, S.-H.; Kim, K.-B.; Shin, K.-H.; Lim, S.N.; Yeon, S.-H. Morphology-controlled graphene nanosheets as anode material for lithium-ion batteries. *Electrochim. Acta* **2014**, *132*, 172–179. [[CrossRef](#)]
142. Shan, H.; Xiong, D.; Li, X.; Sun, Y.; Yan, B.; Li, D.; Lawes, S.; Cui, Y.; Sun, X. Tailored lithium storage performance of graphene aerogel anodes with controlled surface defects for lithium-ion batteries. *Appl. Surf. Sci.* **2016**, *364*, 651–659. [[CrossRef](#)]
143. Zhang, D.; Qian, A.; Chen, J.; Wen, J.; Wang, L.; Chen, C. Electrochemical performances of nano-Co₃O₄ with different morphologies as anode materials for Li-ion batteries. *Ionics* **2012**, *18*, 591–597. [[CrossRef](#)]
144. Zhang, B.; Zhang, Y.; Miao, Z.; Wu, T.; Zhang, Z.; Yang, X. Micro/nano-structure Co₃O₄ as high capacity anode materials for lithium-ion batteries and the effect of the void volume on electrochemical performance. *J. Power Sources* **2014**, *248*, 289–295. [[CrossRef](#)]
145. Yan, X.; Tian, L. Three-Dimensional Crystalline/Amorphous Co/Co₃O₄ Core/Shell Nanosheets as Efficient Electrocatalysts for the Hydrogen Evolution Reaction. *Nano Lett.* **2015**, *15*, 6015–6021. [[CrossRef](#)] [[PubMed](#)]
146. Wang, D.; Yu, Y. Template-Free Synthesis of Hollow-Structured Co₃O₄ Nanoparticles as High-Performance Anodes for Lithium-Ion Batteries. *ACS Nano* **2015**, *9*, 1775–1781. [[CrossRef](#)]
147. Zhou, X.; Shi, J. Microwave irradiation synthesis of Co₃O₄ quantum dots/graphene composite as anode materials for Li-ion battery. *Electrochim. Acta* **2014**, *143*, 175–179. [[CrossRef](#)]
148. Wenelska, K.; Neef, C. Carbon nanotubes decorated by mesoporous cobalt oxide as electrode material for lithium-ion batteries. *Chem. Phys. Lett.* **2015**, *635*, 185–189. [[CrossRef](#)]
149. Wang, H.; Liang, Y. Advanced asymmetrical supercapacitors based on graphene hybrid materials. *Nano Res.* **2011**, *4*, 729–736. [[CrossRef](#)]
150. Guo, C.X.; Wang, M. A Hierarchically Nanostructured Composite of MnO₂/Conjugated Polymer/Graphene for High-Performance Lithium Ion Batteries. *Adv. Energy Mater.* **2011**, *1*, 736–741. [[CrossRef](#)]
151. Gong, Y.; Yang, S. Graphene-Network-Backboned Architectures for High-Performance Lithium Storage. *Adv. Mater.* **2013**, *25*, 3979–3984. [[CrossRef](#)]
152. Wang, H.; Xu, Z. Hybrid Device Employing Three-Dimensional Arrays of MnO in Carbon Nanosheets Bridges Battery-Supercapacitor Divide. *Nano Lett.* **2014**, *14*, 1987–1994. [[CrossRef](#)]
153. Hou, X.; Jiang, H. In Situ Deposition of Hierarchical Architecture Assembly from Sn-Filled CNTs for Lithium-Ion Batteries. *ACS Appl. Mater. Interfaces* **2013**, *5*, 6672–6677. [[CrossRef](#)]
154. Lee, S.-H.; Sridhar, V. Graphene-Nanotube-Iron Hierarchical Nanostructure as Lithium Ion Battery Anode. *ACS Nano* **2013**, *7*, 4242–4251. [[CrossRef](#)]
155. Yan, C.; Chen, G. Template-Based Engineering of Carbon-Doped Co₃O₄ Hollow Nanofibers as Anode Materials for Lithium-Ion Batteries. *Adv. Funct. Mater.* **2016**, *26*, 1428–1436. [[CrossRef](#)]
156. Wang, H.; Mao, N. Cobalt Oxide-Carbon Nanosheet Nanoarchitecture as an Anode for High-Performance Lithium-Ion Battery. *ACS Appl. Mater. Interfaces* **2015**, *7*, 2882–2890. [[CrossRef](#)]
157. Wang, Y.; Yan, F. Onion-like carbon matrix supported Co₃O₄ nanocomposites: A highly reversible anode material for lithium ion batteries with excellent cycling stability. *J. Mater. Chem. A* **2013**, *1*, 5212–5216. [[CrossRef](#)]
158. Wang, G.; Zhu, F. Preparation of Co₃O₄/Carbon Derived from Ionic Liquid and Its Application in Lithium-ion Batteries. *Electrochim. Acta* **2017**, *257*, 138–145. [[CrossRef](#)]
159. Han, Y.; Dong, L. Cobalt oxide modified porous carbon anode enhancing electrochemical performance for Li-ion batteries. *Electrochim. Acta* **2015**, *167*, 246–253. [[CrossRef](#)]
160. Qu, G.; Geng, H. Porous carbon-wrapped mesoporous Co₉S₈ fibers as stable anode for Li-Ion Batteries. *Electrochim. Acta* **2016**, *211*, 305–312. [[CrossRef](#)]
161. Huang, J.; Tang, X.; Liu, K.; Li, Z. Synthesis of porous carbon-coated polycrystalline Co₉S₈ for long-term lithium ion battery. *Mater. Lett.* **2018**, *210*, 88–91. [[CrossRef](#)]
162. Shi, M.; Wang, Q. MOF-derived hollow Co₄S₃/C nanosheet arrays grown on carbon cloth as the anode for high-performance Li-ion batteries. *Dalton Trans.* **2020**, *49*, 14115–14122. [[CrossRef](#)]

163. Wang, L.; Deng, F. Self-confined synthesis of CoS_{1-x} nanoparticles embedded in carbon nanosheets for lithium-ion batteries. *J. Alloy. Compd.* **2021**, *885*, 160947. [[CrossRef](#)]
164. Wu, R. In-situ formation of hollow hybrids composed of cobalt sulfides embedded within porous carbon polyhedra/carbon nanotubes for high-performance lithium-ion batteries. *Adv. Mater.* **2015**, *27*, 3038–3044. [[CrossRef](#)]
165. Zhao, F. Ultrathin mesoporous Co_3O_4 nanosheets-constructed hierarchical clusters as high rate capability and long life anode materials for lithium-ion batteries. *Appl. Surf. Sci.* **2017**, *406*, 46–55.
166. Yin, X.; Wang, Z.; Wang, J.; Yan, G.; Xiong, X.; Li, X.; Guo, H. One-step facile synthesis of porous Co_3O_4 microspheres as anode materials for lithium-ion batteries. *Mater. Lett.* **2014**, *120*, 73–75. [[CrossRef](#)]
167. Tian, D.; Zhou, X.L.; Zhang, Y.H.; Zhou, Z.; Bu, X.H. MOF-Derived Porous Co_3O_4 Hollow Tetrahedra with Excellent Performance as Anode Materials for Lithium-Ion Batteries. *Inorg. Chem.* **2015**, *54*, 8159–8161. [[CrossRef](#)]
168. Jin, Y.; Wang, L. Facile synthesis of monodisperse Co_3O_4 mesoporous microdisks as an anode material for lithium ion batteries. *Electrochim. Acta* **2015**, *151*, 109–117. [[CrossRef](#)]
169. Guo, J.; Chen, L.; Zhang, X.; Chen, H. ChemInform Abstract: Porous Co_3O_4 Nanorods as Anode for Lithium-Ion Battery with Excellent Electrochemical Performance. *J. Solid State Chem.* **2014**, *45*, 193–197. [[CrossRef](#)]
170. Wang, Q.; Jiao, L. CoS_2 Hollow Spheres: Fabrication and Their Application in Lithium-Ion Batteries. *J. Phys. Chem. C* **2011**, *115*, 8300–8304. [[CrossRef](#)]
171. Sennu, P.; Christy, M.; Aravindan, V.; Lee, Y.G.; Nahm, K.S.; Lee, Y.S. Two-Dimensional Mesoporous Cobalt Sulfide Nanosheets as a Superior Anode for a Li-Ion Battery and a Bifunctional Electrocatalyst for the Li-O_2 System. *Chem. Mater.* **2015**, *27*, 5726–5735. [[CrossRef](#)]
172. Song, R.; Dong, Y.; Zhang, D.; Sheng, J.; Yang, S.; Song, H. Nitrogen-Doped Porous Carbon Nanosheets with Ultrahigh Capacity and Quasikapacitive Energy Storage Performance for Lithium and Sodium Storage Applications. *Energy Technol.* **2021**, *9*, 2100309. [[CrossRef](#)]
173. Shi, L.; Chen, Y.; Song, H.; Li, A.; Chen, X.; Zhou, J.; Ma, Z. Preparation and Lithium-Storage Performance of a Novel Hierarchical Porous Carbon from Sucrose Using Mg-Al Layered Double Hydroxides as Template. *Electrochim. Acta* **2017**, *231*, 153–161. [[CrossRef](#)]
174. Xie, Q.; Zhang, Y.; Xie, D.; Zhao, P. EDTA-Fe(III) sodium complex-derived bubble-like nitrogen-enriched highly graphitic carbon nanospheres as anodes with high specific capacity for lithium-ion batteries. *Ionics* **2020**, *26*, 85–94. [[CrossRef](#)]
175. Li, X.; Geng, D.; Zhang, Y.; Meng, X.; Li, R.; Sun, X. Superior cycle stability of nitrogen-doped graphene nanosheets as anodes for lithium ion batteries. *Electrochem. Commun.* **2011**, *13*, 822–825. [[CrossRef](#)]
176. Gu, D.; Li, W.; Wang, F.; Bongard, H.; Spliethoff, B.; Schmidt, W.; Weidenthaler, C.; Xia, Y.; Zhao, D.; Schüth, F. Controllable Synthesis of Mesoporous Peapod-like Co_3O_4 @Carbon Nanotube Arrays for High-Performance Lithium-Ion Batteries. *Angew. Chem. Int. Ed.* **2015**, *54*, 7060–7064. [[CrossRef](#)]
177. Sun, L.; Deng, Q.; Li, Y.; Mi, H.; Wang, S.; Deng, L.; Ren, X.; Zhang, P. $\text{CoO-Co}_3\text{O}_4$ heterostructure nanoribbon/RGO sandwich-like composites as anode materials for high performance lithium-ion batteries. *Electrochim. Acta* **2017**, *241*, 252–260. [[CrossRef](#)]
178. Lu, H.; Qian, R.; Yao, T.; Li, C.; Li, L.; Wang, H. Synthesis of Spherical Carbon-Coated CoP Nanoparticles for High-Performance Lithium-Ion Batteries. *Energy Technol.* **2021**, *9*, 2100605. [[CrossRef](#)]
179. Zhang, X.; Zhao, Y.; Zhang, C.; Wu, C.; Li, X.; Jin, M.; Lan, W.; Pan, X.; Zhou, J.; Xie, E. Cobalt sulfide embedded carbon nanofibers as a self-supporting template to improve lithium ion battery performances. *Electrochim. Acta* **2021**, *366*, 137351. [[CrossRef](#)]